

# Efficient Approximate Degenerate Ordered Statistics Decoding for Quantum Codes via Reliable Subset Reduction

Ching-Feng Kung, Kao-Yueh Kuo, and Ching-Yi Lai

**Abstract**—Efficient decoding of quantum codes is crucial for achieving high-performance quantum error correction. In this paper, we introduce the concept of approximate degenerate decoding and integrate it with ordered statistics decoding (OSD). Previously, we proposed a reliability metric that leverages both hard and soft decisions from the output of belief propagation (BP), which is particularly useful for identifying highly reliable subsets of variables. Using the approach of reliable subset reduction, we reduce the effective problem size. Additionally, we identify a degeneracy condition that allows high-order OSD to be simplified to order-0 OSD. By integrating these techniques, we present an ADOSD algorithm that significantly improves OSD efficiency in the code capacity noise model. We demonstrate the effectiveness of our BP+ADOSD approach through extensive simulations on a variety of quantum codes, including generalized hypergraph-product codes, topological codes, lift-connected surface codes, and bivariate bicycle codes. The results indicate that the BP+ADOSD decoder outperforms existing methods, achieving higher error thresholds and enhanced performance at low error rates. Additionally, we validate the efficiency of our approach in terms of computational time, demonstrating that ADOSD requires, on average, the same amount of time as two to three BP iterations on surface codes at a depolarizing error rate of around 1%. All the proposed algorithms are compared using single-threaded CPU implementations.

## I. INTRODUCTION

Reliable quantum communication is a critical area of research, essential for scaling quantum systems, enabling the exchange of quantum information across distances, and facilitating multiparty protocols. Quantum states are inherently fragile, requiring the implementation of quantum error correction to mitigate the effects of noise and decoherence [2]–[4].

Quantum stabilizer codes, analogous to classical linear block codes, allow efficient encoding and binary syndrome decoding [5]–[7]. A notable class of stabilizer codes is quantum low-density parity-check (LDPC) codes, which are preferred for their high code rates and feasible syndrome measurements from low-weight stabilizers. These codes can be decoded using belief propagation (BP), similar to classical LDPC codes [8]–[20]. A quantum LDPC code of the Calderbank–Shor–Steane

(CSS) type [21], [22] can be decoded by the BP algorithm for binary codes (BP<sub>2</sub>) by treating  $X$  and  $Z$  errors separately. When  $X$  and  $Z$  errors exhibit correlations, such as in depolarizing channels, a quaternary BP algorithm (BP<sub>4</sub>) could be more effective, as it better exploits the error correlations during decoding. An important feature of quantum codes is their binary error syndromes, unlike classical nonbinary codes. Consequently, the complexity of BP<sub>4</sub> can be reduced by restricting message passing in the Tanner graph [13] to scalar messages, which encode the likelihood ratios associated with Pauli commutation relations.

The decoding problem for quantum codes with high degeneracy is particularly challenging for BP, as seen in topological codes [23]–[29]. To address these challenges, several remedies for the BP algorithm have been introduced, including techniques such as random perturbation [9], enhanced feedback [10], [11], check-matrix augmentation [12], message normalization and offset [13], [14], and trapping set analysis [30], [31]. These methods aim to improve the decoding accuracy and convergence of the BP algorithm. A recently developed modified BP<sub>4</sub> algorithm, known as MBP<sub>4</sub>, incorporates additional memory effects and has demonstrated the ability to handle topological codes [32].

We investigate ordered statistic decoding (OSD) as a complementary approach to BP in quantum coding theory. Originally proposed by Fossorier and Lin [33] in classical coding theory for approximating maximum-likelihood decoding [34]–[42], OSD sorts reliability measures of symbols to find probable solutions while maintaining controllable complexity [33], [43]–[46]. Syndrome-based OSD has been used when BP fails to identify a valid error [47] and is particularly effective for degenerate quantum codes [43].

The core operation of OSD is Gaussian elimination on an  $m \times n$  parity-check matrix, identifying unreliable bits with a complexity of  $O(nm^2)$ . Order- $w$  OSD flips up to  $w$  reliable bits to generate error candidates, but this incurs high computational costs. To mitigate complexity, Fossorier *et al.* [47] proposed candidate pruning, and various classical techniques further optimized high-order OSD by reducing the number of candidates examined [48]–[53].

In the quantum regime, OSD-based decoders [43], [44] prioritize less reliable bit-flips, but OSD-0 remains the dominant computational bottleneck. Roffe *et al.* [44] introduced BP2-OSD-CS $\lambda$  with a greedy combination sweep, typically set to  $\lambda = 60$ . iOlius and Martinez [54] proposed the closed-branch (CB) decoder as a lower-complexity alternative,

This article was presented in part at the 2023 International Symposium on Topics in Coding (ISTC) [1].

CYL was supported by the National Science and Technology Council in Taiwan, under Grant Nos. 113-2221-E-A49-114-MY3 and 113-2119-M-A49-008-.

CFK and CYL are with the Institute of Communications Engineering, National Yang Ming Chiao Tung University, Hsinchu 300093, Taiwan. (email: cylai@nycu.edu.tw)

KYK is with the School of Mathematical and Physical Sciences, University of Sheffield, UK.

though BP+CB underperforms BP-OSD-0. Gong *et al.* [55] developed the guided decimation guessing (GDG) decoder, which matches BP2-OSD-CS10 and surpasses BP-OSD-0 for BB codes [56]. To further reduce Gaussian elimination overhead, Wolanski and Barber introduced the ambiguity clustering decoder [57], while Hillmann *et al.* proposed localized statistics decoding (LSD) [58]. Both are divide-and-conquer algorithms, as they partition the decoding problem into smaller subproblems based on specific heuristics.

However, there is a great deal of room for improvement over the current postprocessing techniques in the literature under the code capacity noise model. These methods primarily rely on binary BP to handle quaternary errors, neglecting error correlations, which suggests that binary decoders are inherently suboptimal. In contrast, the quaternary AMBP<sub>4</sub> decoder (the adaptive version of MBP<sub>4</sub>) from [32] has been shown to outperform all the aforementioned decoders across various quantum codes, including topological codes [25], BB codes [56], and generalized hypergraph-product (GHP) codes [43], [44], without requiring postprocessing. For supporting examples, please refer to Figure 7 in Section VI.

OSD serves as a complementary strategy to BP, addressing cases where BP fails. As a result, BP-OSD is naturally expected to outperform AMBP<sub>4</sub>. In this paper, we propose a BP<sub>4</sub>-based OSD to achieve this improvement and introduce an efficient OSD algorithm for quantum codes.

First, the sorting process plays a pivotal role in OSD [33]. For efficient implementation, we consider binary representations of an  $n$ -qubit quantum code and thus an  $n$ -qubit Pauli error variable can be represented by  $2n$  binary variables. Previously we proposed a reliability metric that takes into account the hard-decision history obtained during BP<sub>4</sub> iterations and incorporates soft messages from the last iteration [1]. The  $2n$  binary error variables of an error vector are then sorted according to the reliability metric. Specifically, the length of the last run in a bit's hard-decision history is the primary term in our metric. Through simulations, we demonstrate that incorporating the hard-decision history to determine the reliability order for OSD enhances decoding performance. Our OSD algorithm based on this reliability metric will be denoted as OSD<sub>4</sub>.

To develop an efficient OSD algorithm, it is crucial to reduce the problem size in OSD and minimize the computational burden of Gaussian elimination. To address this challenge, we propose an approach called *reliable subset reduction*. In the code capacity error decoding problem of an  $[[n, k]]$  quantum code, we need to solve a linear system of equations with  $2n$  binary variables and  $n - k$  independent constraints. The core idea is that if the solution for a subset of the variables can be determined with confidence, the linear system can be reduced, thereby lowering the computation burden of both Gaussian elimination and the OSD process. So the primary task is to identify a highly reliable subset. An excellent choice are the bits that exhibit nearly constant hard decision history vectors during BP<sub>4</sub> iterations and show high soft reliability in the final iteration. At low error rates, there is a large portion of highly reliable bits. Eliminating these bits would significantly accelerate the OSD process. Moreover, resources

can be allocated to the less reliable parts, similar to the approaches in [43], [44]. We will demonstrate that in our simulations of surface codes with distances from 11 to 15, the problem sizes are reduced to less than 30% of the original in over 90% of the trials at an error rate of around 2%. We note that the ambiguity clustering decoder [57] and LSD [58] operate at a different stage from our approach, and these algorithms could be applied after reliable subset reduction.

Next, we consider approximate degenerate OSD in quantum codes. A typical OSD generates a list of error candidates for a given error syndrome and selects the one with minimum weight, which is optimal for classical codes. For quantum codes, however, the optimal decoding criterion involves choosing the error coset with the highest probability, a criterion that is challenging to implement in practice. To address this, we consider approximate degenerate decoding in OSD by focusing only on relatively low-weight terms within a coset.

Additionally, we introduce a degenerate error candidate pruning condition for stabilizer codes. We show that certain bit-flips in OSD correspond to multiplying stabilizers, resulting in degenerate error candidates. These bit-flips may alter the error weight but do not change the error coset, allowing them to be ignored in approximate degenerate OSD. To improve OSD efficiency, the minimum weight decoding criterion is applied. A key observation is that if all bit-flips correspond to multiplying a stabilizer, high-order OSD is unnecessary. We note that a degeneracy condition is also utilized in ambiguity clustering to facilitate subproblem resolution [57].

Integrating all the mentioned techniques, we propose an approximate degenerate OSD algorithm, abbreviated as ADOSD<sub>4</sub>. We conduct simulations of MBP<sub>4</sub> and our OSD schemes OSD<sub>4</sub> and ADOSD<sub>4</sub> on several quantum codes under depolarizing errors in the code capacity noise model, including BB codes [56], rotated toric codes and rotated surface codes [25], (6.6.6) and (4.8.8) color codes [28], twisted XZZX codes on a torus [59], GHP codes [43], [44], and lift-connected surface (LCS) codes [60].

The results demonstrate that our proposed schemes outperform previous approaches in the literature, both in terms of error thresholds for topological codes and low error rate performance (logical error rate around  $10^{-6}$ ). Our MBP<sub>4</sub>+OSD<sub>4</sub> and MBP<sub>4</sub>+ADOSD<sub>4</sub> decoders outperform other binary BP-OSD schemes in these quantum codes. We achieve thresholds of approximately 17.5%–17.7% for the toric, surface, and twisted XZZX codes, and thresholds of 15%–15.42% for the (4.8.8) and (6.6.6) color codes, as summarized in Table III. They even surpass the minimum weight perfect matching (MWPM) decoder on surface and toric codes [69], [70].

Finally, we analyze the time efficiency of our OSD schemes for these quantum codes using single-threaded CPU implementations. The simulation results, summarized in Table IV, show that the time consumption of ADOSD<sub>4</sub> for surface codes with distances from 11 to 15 is approximately 2% to 4% of that for order-2 OSD<sub>4</sub> with similar decoding performance at logical error rate around  $10^{-6}$ . Moreover, the average time consumption per codeword for ADOSD<sub>4</sub> is approximately equivalent to 2 to 3 BP<sub>4</sub> iterations, whereas a successful BP trial typically takes 2 to 3 iterations on average. This suggests

that ADOSD<sub>4</sub> is an excellent complement to BP, especially since ADOSD<sub>4</sub> is used only when BP fails.

This paper is organized as follows. We introduce stabilizer codes in Section II. Section III discusses reliability metrics and the associated OSD algorithm. The reliable subset reduction method is presented in Section IV. We then cover approximate degenerate decoding in Section V, and provide simulation results in Section VI. Finally, we conclude in Sec. VII.

## II. QUANTUM STABILIZER CODES

In this section, we review the basic of stabilizer codes and define the relevant notation [5]–[7].

Let  $I = \begin{bmatrix} 1 & 0 \\ 0 & 1 \end{bmatrix}$ ,  $X = \begin{bmatrix} 0 & 1 \\ 1 & 0 \end{bmatrix}$ ,  $Z = \begin{bmatrix} 1 & 0 \\ 0 & -1 \end{bmatrix}$ , and  $Y = iXZ$  denote the Pauli matrices. The  $n$ -fold Pauli group,  $\mathcal{G}_n$ , is the group of  $n$ -qubit Pauli operators, defined as

$$\mathcal{G}_n \triangleq \{\omega M_1 \otimes \cdots \otimes M_n : \omega \in \{\pm 1, \pm i\}, M_j \in \{I, X, Y, Z\}\}.$$

Every nonidentity Pauli operator in  $\mathcal{G}_n$  has eigenvalues  $\pm 1$ . Any two Pauli operators either commute or anticommute with each other. The weight of a Pauli operator  $g \in \mathcal{G}_n$ , denoted  $\text{wt}(g)$ , refers to the number of its nonidentity components.

We consider Pauli errors, assuming independent depolarizing errors with rate  $\epsilon$ . Each qubit independently experiences an  $X$ ,  $Y$ , or  $Z$  error with probability  $\epsilon/3$  and no error with probability  $1 - \epsilon$ . Therefore, at a small error rate  $\epsilon$ , low-weight Pauli errors are more likely to occur across  $n$  qubits.

A *stabilizer group*  $\mathcal{S}$  is an Abelian subgroup in  $\mathcal{G}_n$  such that  $-I^{\otimes n} \notin \mathcal{S}$  [7]. Suppose that  $\mathcal{S}$  is generated by  $n - k$  independent generators. Then  $\mathcal{S}$  defines an  $[[n, k, d]]$  stabilizer code  $\mathcal{C}(\mathcal{S})$  that encodes  $k$  logical qubits into  $n$  physical qubits:

$$\mathcal{C}(\mathcal{S}) = \{|\psi\rangle \in \mathbb{C}^{2^n} : g|\psi\rangle = |\psi\rangle, \forall g \in \mathcal{S}\}.$$

The elements in  $\mathcal{S}$  are called *stabilizers*. The parameter  $d$  represents the minimum distance of the code such that any Pauli error of weight less than  $d$  is *detectable*.

An error  $e \in \mathcal{G}_n$  can be detected by  $\mathcal{C}(\mathcal{S})$  through stabilizer measurements if  $e$  anticommutes with some of the stabilizers. Suppose that  $\{g_i\}_{i=1}^m$ , where  $m \geq n - k$ , is a set of stabilizers that generates  $\mathcal{S}$ . Their binary measurement outcomes are referred to as the *error syndrome* of  $e$ . Let  $N(\mathcal{S}) \subset \mathcal{G}_n$  denote the normalizer group of  $\mathcal{S}$ , which consists of the Pauli operators that commute with all stabilizers. Consequently, if an error is in  $N(\mathcal{S})$ , it will have zero syndrome and cannot be detected. Note that if an error is a stabilizer, it has no effect on the code space. An element in the normalizer group  $N(\mathcal{S})$  that is not a stabilizer, up to a phase, is called a *nontrivial logical operator as it changes the logical state of a code*. Therefore, the minimum distance of  $\mathcal{C}(\mathcal{S})$  is defined as the minimum weight of a nontrivial logical operator. It can be observed that  $e \in \mathcal{G}_n$  and  $eg$  for  $g \in \mathcal{S}$  have the same effects on the codespace. They are called *degenerate* to each other. We say that a quantum code is *highly degenerate* if it has many stabilizers with low weight relative to its minimum distance.

A syndrome decoding problem can be stated as follows: given an error syndrome of an unknown Pauli error  $e$ , find the most probable  $\hat{e} \in \mathcal{G}_n$  that matches the syndrome. An

error estimate  $\hat{e}$  is considered *valid* if it matches the syndrome or  $\hat{e}e \in \mathcal{S}$ . Two decoding criteria are typically considered: minimum weight decoding and degenerate maximum likelihood decoding [61]–[63]. In minimum weight decoding, the error  $\hat{e}$  with the smallest weight is chosen, while in degenerate maximum likelihood decoding, the error  $\hat{e}$  whose coset  $\hat{e}\mathcal{S}$  has the minimum coset probability is selected. However, degenerate maximum likelihood decoding has exponential complexity and is impractical due to the need for coset enumeration. We propose the following criterion.

**Definition 1.** (Approximate Degenerate Decoding)

A  $\delta$ -approximate degenerate decoding ( $\delta$ -ADD) criterion aims to find an error estimate  $\hat{e}$  that matches the given syndrome, maximizing the dominant terms of its coset probability

$$\sum_{g \in \mathcal{S}, \text{wt}(g) \leq \delta} \Pr\{\hat{e}g\}. \quad (1)$$

Note that 0-ADD reduces to minimum weight decoding, while  $n$ -ADD corresponds precisely to degenerate maximum likelihood decoding.

### A. Binary representations

We can study the decoding problem in the binary vector space [5], [7], using a mapping  $\varphi : \mathcal{G}_1 \rightarrow \{0, 1\}^2$

$$I \mapsto [0 \mid 0], X \mapsto [1 \mid 0], Z \mapsto [0 \mid 1], Y \mapsto [1 \mid 1].$$

We extend the  $\varphi$  to  $\mathcal{G}_n$  as follows: For  $g = M_1 \otimes M_2 \otimes \cdots \otimes M_n \in \mathcal{G}_n$ ,

$$\varphi(g) \triangleq \mathbf{g} = [\mathbf{g}^X \mid \mathbf{g}^Z] = [\mathbf{g}_1^X \cdots \mathbf{g}_n^X \mid \mathbf{g}_1^Z \cdots \mathbf{g}_n^Z],$$

where  $\mathbf{g}^X \in \{0, 1\}^n$  and  $\mathbf{g}^Z \in \{0, 1\}^n$  are the indicator vectors of  $X$  and  $Z$  components of  $g$ , respectively, such that  $[\mathbf{g}_j^X \mid \mathbf{g}_j^Z] = \varphi(M_j)$ .

A *check matrix* of  $\mathcal{C}(\mathcal{S})$  corresponding a set of stabilizer generators  $\{g_i\}_{i=1}^m$  is an  $m \times 2n$  binary matrix  $\mathbf{H}$  with rows  $\varphi(g_1), \dots, \varphi(g_m)$ .

An error  $e \in \mathcal{G}_n$  can be represented by  $\mathbf{e} = \varphi(e)$  and its error syndrome is

$$\mathbf{s} = \mathbf{H}\mathbf{e}^\top \in \{0, 1\}^{m \times 1}, \quad (2)$$

where  $\mathbf{e}^\top$  denotes the transpose of  $\mathbf{e}$ ,  $\Lambda = \begin{bmatrix} \mathbf{0} & \mathbf{I}_n \\ \mathbf{I}_n & \mathbf{0} \end{bmatrix}$ ,  $\mathbf{I}_n$  is the  $n \times n$  identity matrix, and  $\mathbf{0}$  is the zero matrix of appropriate dimensions.

Suppose this code has  $2k$  independent logical operators,  $\bar{X}_i$  and  $\bar{Z}_j$  for  $i, j = 1, \dots, k$ , which, together with the stabilizers  $\{g_i\}$ , generate the normalizer group  $N(\mathcal{S})$ . The  $2k \times 2n$  binary logical matrix  $\mathbf{L}$  is defined with rows  $\varphi(\bar{X}_1), \dots, \varphi(\bar{X}_k), \varphi(\bar{Z}_1), \dots, \varphi(\bar{Z}_k)$ . Since stabilizers commute with logical operators, we have  $\mathbf{H}\mathbf{L}^\top = \mathbf{0}$ .

The decoding problem is to solve the system of linear equations (2) with  $2n$  binary variables in  $\mathbf{e} \in \{0, 1\}^{2n}$  that are most probable. Note that  $\mathbf{H}$  is of rank  $n - k$  so the degree of freedom of this binary system is  $n + k$ .

An error  $e \in \mathcal{G}_n$  is classified as a logical error for a decoder if the decoder fails or outputs  $\hat{e} \in \mathcal{G}_n$  such that

$$\mathbf{H}\mathbf{L}(\mathbf{e} + \hat{\mathbf{e}})^\top = \mathbf{0} \quad (3)$$

but

$$\mathbf{L}\Lambda(\mathbf{e} + \hat{\mathbf{e}})^\top \neq \mathbf{0}. \quad (4)$$

### B. Belief Propagation (BP) Decoding

We explain how a quaternary BP algorithm works in the following [13], which is computed in linear domain. A log-likelihood version of BP can be found in [14].

Given a check matrix  $\mathbf{H}$ , a syndrome  $\mathbf{s}$ , and a depolarizing error rate  $\epsilon$ , BP performs the following steps:

- 1) An initial error distribution  $\mathbf{p}_i \in \mathbb{R}^4$  for qubit  $i \in \{1, 2, \dots, n\}$  is chosen for BP.
- 2) The belief distribution vector  $\mathbf{q}_i = (q_i^I, q_i^X, q_i^Y, q_i^Z)$  will be updated by BP, using the messages of parity-check satisfaction and the channel statistics  $\mathbf{p}_i$  for  $i = 1, 2, \dots, n$ .
- 3) At each iteration, an error estimate  $\hat{\mathbf{e}} \in \{0, 1\}^{2n}$  is made according to the hard decision on  $\mathbf{q}_i$ . If a valid error estimate is generated, it will be accepted as the solution; otherwise, go to the next iteration starting from step 2).

Steps 2) and 3) will be iterated for a maximum number of  $T$  iterations, where  $T$  is chosen in advance. If no valid estimate is obtained after  $T$  iterations, BP will claim a failure.

## III. ORDER-STATISTIC DECODING BASED ON QUATERNARY BELIEF PROPAGATION

In the aforementioned syndrome decoding problem, we aim to solve a system of linear equations given by (2), for a given parity-check matrix  $\mathbf{H}$  and an error syndrome  $\mathbf{s}$  with  $2n$  binary variables in  $\mathbf{e}$ . The linear system has  $n - k$  independent constraints, implying that there are  $n + k$  degrees of freedom in the vector  $\mathbf{e}$ . Given the values of these  $n + k$  bits, one can reconstruct  $\mathbf{e}$ . If BP fails to provide a valid error estimate after  $T$  iterations, OSD will be utilized.

In the context of OSD, a critical step involves identifying and sorting the accurate and reliable coordinates to establish  $n + k$  linearly independent bits. Then, we can use these coordinates to generate a valid error that matches the syndrome. To accomplish this, it is necessary to establish the concept of reliability order as a means of prioritizing the coordinates based on their reliability.

### A. Reliability order based on $BP_4$

To utilize the quaternary distribution generated by  $BP_4$  for each qubit error in OSD, we propose a method that employs the hard-decision history from all BP iterations and the output probabilities from the last BP iteration.

Suppose that BP fails to provide a valid error after a maximum of  $T$  iterations. At this point, we have the output distribution  $\mathbf{q}_i = (q_i^I, q_i^X, q_i^Y, q_i^Z)$ ,  $i = 1, 2, \dots, n$  from the last BP iteration. Additionally, we have the hard-decision results for all  $T$  iterations, denoted by  $\mathbf{h}_i^{(j)} \in \{I, X, Y, Z\}$  for  $i = 1, \dots, n$  and  $j = 1, \dots, T$ . For example,  $\mathbf{h}_i^{(1)}, \mathbf{h}_i^{(2)}, \dots, \mathbf{h}_i^{(T)}$  represent the hard-decision result history of BP at qubit  $i$  and  $\mathbf{h}_1^{(j)}, \mathbf{h}_2^{(j)}, \dots, \mathbf{h}_n^{(j)}$  represent the hard-decision results of BP at the  $j$ -th iteration.

Our objective is to assign reliability for each Pauli  $X$  and  $Z$  error. Following the reliability definitions in [1], [43], we define two types of measures in the following.

**Definition 2.** Define a *hard-decision reliability vector*  $\boldsymbol{\eta} = (\eta_1, \dots, \eta_n) \in \mathbb{Z}^n$  such that  $\eta_i$  represents the number of consecutive iterations during which the error at qubit  $i$  remains unchanged until the final hard decision is made.

In other words,  $\eta_i$  is the length of the last run in the string  $\mathbf{h}_i^{(1)}, \mathbf{h}_i^{(2)}, \dots, \mathbf{h}_i^{(T)}$ . For example, if the hard-decision outputs at the first qubit over the last five iterations are  $X, Y, Z, Z, Z$ , then the final hard decision output is  $Z$  and  $\eta_1 = 3$ . This means that the error at qubit 1 persisted unchanged as  $Z$  for three iterations when BP stops.

When BP fails, the belief distributions  $\mathbf{q}_i = (q_i^I, q_i^X, q_i^Y, q_i^Z)$  will be utilized in the reliability measure.

**Definition 3.** Define two *soft reliability functions*

$$\begin{aligned} \phi^X(i) &= \max\{q_i^X + q_i^Y, q_i^I + q_i^Z\}, \\ \phi^Z(i) &= \max\{q_i^Z + q_i^Y, q_i^I + q_i^X\}, \end{aligned}$$

for  $i \in \{1, 2, \dots, n\}$ .

Note that  $\{q_i^X + q_i^Y, q_i^I + q_i^Z\}$  is a binary distribution indicating the likelihood of an  $X$  error occurring at the  $i$ -th qubit and similarly for  $\{q_i^X + q_i^Y, q_i^I + q_i^Z\}$ .

Our modified  $BP_4$  algorithm is presented in Algorithm 1.

---

#### Algorithm 1 $BP_4$

---

**Input:** check matrix  $\mathbf{H} \in \{0, 1\}^{m \times 2n}$ , syndrome  $\mathbf{s} \in \{0, 1\}^{m \times 1}$ , error rate  $\epsilon$ , maximum number of iterations  $T$ .

**Output:** A valid error estimate  $\hat{\mathbf{e}} \in \{0, 1\}^{2n}$ , belief distributions  $\{\mathbf{q}_i\}_{i=1}^n$  and hard-decision reliability vector  $\boldsymbol{\eta} \in \mathbb{Z}^n$ .

**Initialization:**

Choose initial error distributions  $\mathbf{p}_i \in \mathbb{R}^4$  for  $i = 1, \dots, n$ .  
 Let  $\eta_i = 1$  for  $i = 1, \dots, n$ . Let  $\mathbf{h}_i = I$  for  $i = 1, \dots, n$ .  
 Let  $\mathbf{q}_i = \mathbf{0}$  for  $i = 1, \dots, n$ .

**Steps:**

**for**  $j = 1$  to  $T$  **do**

Update  $\{\mathbf{q}_i\}_{i=1}^n$ , using  $\mathbf{H}, \mathbf{s}$ , and  $\{\mathbf{p}_i\}_{i=1}^n$ .

**for**  $i = 1$  to  $n$  **do**

**if**  $\mathbf{h}_i = \text{HardDecision}(\mathbf{q}_i)$  **then**  $\eta_i \leftarrow \eta_i + 1$ ;

**else**  $\mathbf{h}_i \leftarrow \text{HardDecision}(\mathbf{q}_i)$ .  $\eta_i = 1$ .

**end if**

**end for**

**if** the hard-decision  $\mathbf{h}$  matches the syndrome  $\mathbf{s}$  **then**

**return** "Success" and  $\varphi(\mathbf{h})$ .

**end if**

**end for**

**return** "Failure",  $\{\mathbf{q}_i\}_{i=1}^n$ , and  $\boldsymbol{\eta}$ . ▷ BP fails.

---

Now we define a reliability order for the bits in  $\mathbf{e} = [\mathbf{e}^X \mid \mathbf{e}^Z] \in \{0, 1\}^{2n}$  based on the outputs of  $BP_4$ , using the aforementioned hard and soft reliability functions.

**Definition 4.** For  $1 \leq i, j \leq n$  and  $a, b \in \{X, Z\}$ , error bit  $\mathbf{e}_i^a$  is said to be *more reliable* than error bit  $\mathbf{e}_j^b$  if  $\eta_i > \eta_j$ , or if  $\phi^a(i) \geq \phi^b(j)$  when  $\eta_i = \eta_j$ .

This definition means that the hard-decision history reliability is used to rank the error coordinates, with the soft reliability serving as a tie-breaker.

Let  $\tilde{\mathbf{e}}$  be the hard-decision output from  $\text{BP}_4$  after  $T$  iterations. If  $\tilde{\mathbf{e}}$  does not match the syndrome, OSD will be applied. We now present our OSD algorithm based on the reliability orders as in Algorithm 2, which is referred to as  $\text{OSD}_4\text{-}0$ .

---

**Algorithm 2**  $\text{OSD}_4\text{-}0$ 


---

**Input:** check matrix  $\mathbf{H} \in \{0, 1\}^{m \times 2n}$  of rank  $n - k$ , syndrome  $\mathbf{s} \in \{0, 1\}^{m \times 1}$ , hard-decision reliability vector  $\boldsymbol{\eta} \in \mathbb{Z}^n$ , hard-decision vector  $\tilde{\mathbf{e}} \in \{0, 1\}^{2n}$ , and belief distributions  $\{\mathbf{q}_i\}_{i=1}^n$ .

**Output:** A valid error estimate  $\hat{\mathbf{e}} \in \{0, 1\}^{2n}$ .

**Steps:**

- 1: Sort the error bits in ascending order of reliability. Construct a column permutation function  $\pi$  corresponding to the sorting order. Calculate  $\pi(\tilde{\mathbf{e}})$  and  $\pi(\mathbf{H}\boldsymbol{\Lambda})$ .
- 2: Perform Gaussian elimination on  $\pi(\mathbf{H}\boldsymbol{\Lambda})$  and let the output be denoted by  $R(\pi(\mathbf{H}\boldsymbol{\Lambda}))$ , where  $R$  represents the corresponding row operations in the Gaussian elimination. If necessary, apply a column permutation function  $\mu$  to ensure that the first  $n - k$  columns of the resulting matrix are linearly independent. Thus we have

$$\mu(R(\pi(\mathbf{H}\boldsymbol{\Lambda}))) = \begin{bmatrix} \mathbf{I}_{n-k} & \mathbf{A} \\ \mathbf{0} & \mathbf{0} \end{bmatrix}, \quad (5)$$

for some  $\mathbf{A} \in \{0, 1\}^{(n-k) \times (n+k)}$ , where the last  $m - (n - k)$  rows are all zeros.

- 3: Let  $\mathbf{s}' = R(\mathbf{s})$  so that the parity-check condition (2) becomes

$$\mathbf{s}' = \mu(R(\pi(\mathbf{H}\boldsymbol{\Lambda}))) (\mu(\pi(\mathbf{e})))^\top. \quad (6)$$

Remove the last  $m - (n - k)$  entries of  $\mathbf{s}'$ .

- 4: Let  $\mu(\pi(\tilde{\mathbf{e}})) = [\tilde{\mathbf{e}}^U \ \tilde{\mathbf{e}}^R]$ , where  $\tilde{\mathbf{e}}^U$  represents the independent and unreliable subset of  $n - k$  bits and  $\tilde{\mathbf{e}}^R$  is the reliable subset of  $n + k$  bits. Use the reliable subset  $\tilde{\mathbf{e}}^R$  and the modified parity-check condition 6 to select feasible unreliable bits

$$\tilde{\mathbf{e}}^U = \mathbf{s}'^\top \oplus \tilde{\mathbf{e}}^R \mathbf{A}^\top. \quad (7)$$

**return**

$$\hat{\mathbf{e}} \triangleq \pi^{-1} \left( \mu^{-1} \left( \left[ \mathbf{s}'^\top \oplus \tilde{\mathbf{e}}^R \mathbf{A}^\top \quad \tilde{\mathbf{e}}^R \right] \right) \right). \quad (8)$$


---

We also define a reliability order that accounts for only the soft reliability functions of  $\text{BP}_4$ .

**Definition 5.** Error bit  $\mathbf{e}_i^a$  is said to be *more reliable* than error bit  $\mathbf{e}_j^b$  in the marginal distribution if  $\phi^a(i) \geq \phi^b(j)$ .

The OSD based on Definition 5 is referred to as  $\text{mOSD}_4$ . Other alternative metrics can also be considered, such as

$$\text{(Entropy)} \quad H_4(\mathbf{q}_i) = - \sum_{M \in \{I, X, Y, Z\}} q_i^M \log(q_i^M), \quad (9)$$

$$\text{(Max)} \quad \max(\mathbf{q}_i) = \max_{M \in \{I, X, Y, Z\}} q_i^M. \quad (10)$$

The reliability of qubit  $i$  is assessed based on the quaternary entropy of its belief distribution  $\mathbf{q}_i$  (Entropy) or based on the maximum probability of the distribution (Max). For our purpose, the hard-decision output of BP is first sorted in the Pauli basis based on the reliability metric (either Entropy or Max) and then transformed into a binary vector for OSD [43]. We will compare these reliability metrics in Section VI-D.

### B. $\text{OSD}_4\text{-}w$

If some bits in the reliable subset are incorrect, additional processing is necessary. We may flip up to  $w$  bits in the reliable subset and generate the corresponding error estimate. If this error estimate is valid, it is an error candidate. This process is repeated for all  $\sum_{i=0}^w \binom{n+k}{i}$  possibilities, and the output will be a valid error candidate that is optimal with respect to  $\delta$ -ADD for a certain  $\delta$ . This type of OSD algorithm is referred to as order- $w$   $\text{OSD}_4$  (or  $\text{OSD}_4\text{-}w$  for short).

In order to explore all  $\sum_{i=0}^w \binom{n+k}{i}$  possibilities, we propose to use the depth-first search (DFS) algorithm. Figure 1 illustrates the idea of using DFS to traverse all bit strings of length 4 and with weight at most 2. One can see that a child node is obtained by flipping one zero bit from its parent node. Consequently, one can recursively generate all  $\sum_{i=0}^w \binom{n+k}{i}$  possibilities by bit flipping and encoding.

**Lemma 6.** Given an  $\text{OSD}_4\text{-}0$  output vector, flipping one of its reliable bits to generate an error candidate takes time  $O(n)$ . Similarly, generating an error candidate corresponding to a child node from its parent node also takes  $O(n)$  time.

*Proof.* Consider the vector  $[\mathbf{s}'^\top \oplus \mathbf{e}^R \mathbf{A}^\top \mid \tilde{\mathbf{e}}_1^R \tilde{\mathbf{e}}_2^R \cdots \tilde{\mathbf{e}}_{n+k}^R]$  generated by  $\text{OSD}_4\text{-}0$  in (8), where  $\tilde{\mathbf{e}}_j^R$  are reliable bits. Suppose that the matrix  $\mathbf{A}$  in (5) has columns  $\mathbf{A}_1, \mathbf{A}_2, \dots, \mathbf{A}_{n+k} \in \{0, 1\}^{n-k}$ . Then according to (7), flipping the bit  $\tilde{\mathbf{e}}_i^R$  corresponds to adding the  $\text{OSD}_4\text{-}0$  output by the vector

$$[\mathbf{A}_j^\top \ 0 \cdots 0 \ 1 \ 0 \cdots 0] \in \{0, 1\}^{2n}, \quad (11)$$

where  $\mathbf{A}_j$  is the  $j$ -th column of  $\mathbf{A}$ , and generating the vector

$$[\mathbf{s}'^\top \oplus \tilde{\mathbf{e}}^R \mathbf{A}^\top \oplus \mathbf{A}_i^\top \mid \tilde{\mathbf{e}}_1^R \tilde{\mathbf{e}}_2^R \cdots (1 \oplus \tilde{\mathbf{e}}_i^R) \cdots \tilde{\mathbf{e}}_{n+k}^R], \quad (12)$$

which is a valid error candidate after permutations. This calculation takes  $O(n)$  time.  $\square$

To efficiently navigate through these possibilities, we can utilize the technique described in Lemma 6 combining with the DFS algorithm. Then all  $\sum_{i=0}^w \binom{n+k}{i}$  candidates can be recursively generated.

### C. Complexity of $\text{OSD}_4$

We analyze the complexity of OSD based on 0-ADD in the following. The complexity of  $\text{OSD}_4\text{-}0$  is dominated by the Gaussian elimination step, which is then  $O(2nm^2) = O(n^3)$ , assuming  $m = O(n)$ . For  $\text{OSD}_4\text{-}w$  with  $w > 0$ , the total number of possible flips is  $\sum_{j=0}^w \binom{n+k}{j}$ , which can be expressed as  $O((n+k)^w)$  or simply  $O(n^w)$ .

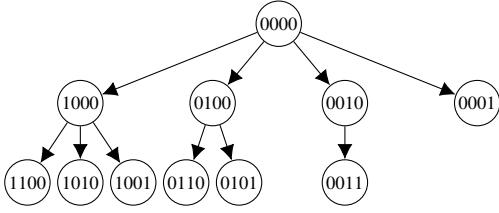


Fig. 1: A tree with nodes consisting of all bit strings of length 4 and with at most weight 2. The root node is 0000. A child node is obtained by flipping one of the zero bits from its parent node that come after the last bit that is one.

In Lemma 6, when we flip a bit in the reliable part, it requires only  $O(n)$  calculations to find an error candidate. Additionally, by running through  $\sum_{j=0}^w \binom{n+k}{j}$  possibilities using the DFS algorithm, the  $\text{OSD}_{4-w}$  algorithm has a complexity of  $O(n^3 + n^{w+1})$ , which simplifies to  $O(n^3)$  when  $w \leq 2$ .

---

### Algorithm 3 HRSR

---

**Input:** check matrix  $\mathbf{H} \in \{0, 1\}^{m \times 2n}$  of rank  $n-k$ , syndrome  $\mathbf{s} \in \{0, 1\}^{m \times 1}$ , hard-decision reliability vector  $\boldsymbol{\eta} \in \mathbb{Z}^n$ , hard-decision vector  $\mathbf{e} \in \{0, 1\}^{2n}$ , belief distributions  $\{\mathbf{q}_i\}_{i=1}^n$ , and soft reliability threshold  $\theta$ .

**Output:** shortened variables  $\tilde{\mathbf{s}}, \tilde{\mathbf{H}}, \mathbf{e}^H$ , and  $\sigma$ .

**Steps:**

- 1: Use  $\boldsymbol{\eta}, \mathbf{q}_{i=1}^n$ , and  $\theta$  to identify the highly reliable bits in  $\mathbf{e}$  based on Definition 7. Assume that there are  $v$  such highly reliable bits.
- 2: Let  $\sigma$  be a column permutation such that  $\sigma(\mathbf{e}) = [\mathbf{e}' \ \mathbf{e}^H]$ , where  $\mathbf{e}^H$  is the highly reliable subset of  $v$  bits, and  $\mathbf{e}'$  is the remaining  $2n-v$  bits. Let  $\sigma(\hat{\mathbf{e}}) = [\hat{\mathbf{e}}' \ \mathbf{e}^H]$  be a permuted error estimate, which contains the highly reliable bits in  $\mathbf{e}^H$ .
- 3: Let  $\tau$  be a row permutation such that  $\tau(\sigma(\mathbf{H}\boldsymbol{\Lambda})) = \begin{bmatrix} \tilde{\mathbf{H}} & \mathbf{B} \\ \mathbf{0} & \mathbf{C} \end{bmatrix}$  for  $\tilde{\mathbf{H}} \in \{0, 1\}^{m' \times (2n-v)}$  with  $m' \leq m$ . The  $m-m'$  rows  $[\mathbf{0} \ \mathbf{C}]$  correspond to parity checks related only to the highly reliable bits. Assume that  $\tau(\mathbf{s}) = \begin{bmatrix} \mathbf{s}'' \\ \mathbf{s}^H \end{bmatrix}$ , where  $\mathbf{s}'' \in \{0, 1\}^{m' \times 1}$ , and  $\mathbf{s}^H \in \{0, 1\}^{(m-m') \times 1}$  are the syndrome bits corresponding to  $[\mathbf{0} \ \mathbf{C}]$ .
- 4: Verify the parity check condition related to the highly reliable bits.

**if**  $\mathbf{s}^H \neq \mathbf{C}(\mathbf{e}^H)^\top$  **then return** "Failure";  
**else** we have a new parity-check condition

$$\tilde{\mathbf{s}} = \tilde{\mathbf{H}}(\hat{\mathbf{e}}')^\top, \quad (13)$$

where  $\tilde{\mathbf{s}} = \mathbf{s}'' - \mathbf{B}(\mathbf{e}^H)^\top$ .

**if** (13) is solvable **then return**  $\tilde{\mathbf{s}}, \tilde{\mathbf{H}}, \mathbf{e}^H$ , and  $\sigma$ ;  
**else return** "Failure".

**end if**

**end if**

---

## IV. HIGHLY RELIABLE SUBSET REDUCTION

As we increase the order  $w$  of OSD, we can expect an improvement in the decoder's performance. In particular, when  $w = n+k$  and  $\delta = n$ ,  $\text{OSD}_{4-(n+k)}$  using  $n$ -ADD becomes a maximum likelihood decoder. However, increasing the order  $w$  also leads to an increase in time complexity.

To address this issue, we propose an approach to reduce the problem size for OSD. Recall that OSD is used to solve a linear system with  $2n$  binary variables and  $n-k$  constraints. If a subset of binary variables is known, the problem size—and consequently the computational complexity—can be reduced. The number of binary variables in the reduced linear system is referred to as the *effective length* for OSD, which corresponds to the length of the remaining binary error variable vector. We have the following definition of highly reliable coordinates.

**Definition 7.** An error bit  $\mathbf{e}_i^a$ , where  $i \in 1, \dots, n$  and  $a \in X, Z$ , is considered *highly reliable* if its hard-decision reliability equals  $T$  or  $T+1$ , and its soft reliability  $\phi^a(i)$  satisfies  $\phi^a(i) \geq \theta$ , where  $\theta$  is a predetermined reliability threshold.

An error variable has hard reliability  $T$  if BP has a constant output at all iterations; a hard reliability of  $T+1$  means the corresponding error variable is the identity during the BP process after being initialized to the identity. The soft reliability threshold  $\theta$  is chosen close to one to ensure that a highly reliable coordinate not only exhibits an almost constant hard-decision history but also has a high soft reliability value.

These highly reliable variables are crucial in the OSD process. Identifying these variable nodes allows us to greatly reduce the computation burden of OSD.

These highly reliable parts provide outcomes that can be trusted and will remain unchanged throughout the  $\text{OSD}_4$  procedure with high probability. Consequently, we propose to exclude these highly reliable parts from the parity check relations. By doing so, we can avoid unnecessary calculations and prioritize our focus on the unreliable part. Our highly reliable subset reduction (HRSR) algorithm is given in Algorithm 3.

Equation (13) follows from the parity-check condition (2) with

$$\begin{bmatrix} \mathbf{s}'' \\ \mathbf{s}^H \end{bmatrix} = \tau(\sigma(\mathbf{H}\boldsymbol{\Lambda}))[\hat{\mathbf{e}}' \ \mathbf{e}^H]^\top = \begin{bmatrix} \tilde{\mathbf{H}}(\hat{\mathbf{e}}')^\top + \mathbf{B}(\mathbf{e}^H)^\top \\ \mathbf{C}(\mathbf{e}^H)^\top \end{bmatrix}$$

and the conditions  $\mathbf{s}^H = \mathbf{C}(\mathbf{e}^H)^\top$  and  $\tilde{\mathbf{s}} = \mathbf{s}'' - \mathbf{B}(\mathbf{e}^H)^\top$ .

If HRSR returns a reduced linear system as in (13), we then use  $\text{OSD}_{4-w}$  to solve it with hard-decision BP output  $\mathbf{e}'$  and corresponding reliabilities  $\boldsymbol{\eta}, \phi^X$ , and  $\phi^Z$ . Suppose that  $\text{OSD}_{4-w}$  returns  $\hat{\mathbf{e}}'$ . Then the error estimate is  $\sigma^{-1}([\hat{\mathbf{e}}' \ \mathbf{e}^H]^\top)$ .

Reducing the problem size may cause the reduced check matrix to lose the ability to represent all valid codewords if its dimension becomes too small. To address this, in Step 4 of Algorithm 3, we verify that the removed highly reliable bits align with the corresponding syndrome bits. If they do not, the algorithm reports a failure.

This method effectively reduces the overhead in OSD, especially at low error rates as will be shown in the simulation section. Furthermore, as the effective length in OSD

is reduced, we can apply higher order OSD if only a fixed amount of computation is allowed. Consider, for instance, the case where the number of error candidates to be tested in OSD is  $\Gamma$ . For the original decoding problem, OSD<sub>4-2</sub> has

$$\Gamma = \binom{n+k}{0} + \binom{n+k}{1} + \binom{n+k}{2}. \quad (14)$$

Using the HRSR algorithm for  $v$  highly reliable bits, we have a reduced system of linear equations with  $2n - v$  binary variables. Assume the rank of the reduced system is  $n - k - (m - m')$ . Then we can apply OSD<sub>4- $w$</sub>  under the constraint of  $\Gamma$  candidates, with  $w$  given by

$$w = \arg \max_x \sum_{i=0}^x \binom{n+k-v+(m-m')}{i} \leq \Gamma. \quad (15)$$

Note that even though the number of tested candidates is fixed, the complexity of OSD following the HRSR algorithm is lower due to the reduced effective length.

## V. APPROXIMATE DEGENERATE OSD

In this section, we discuss how degeneracy in quantum codes helps reduce the computation of OSD. Recall that in OSD- $w$ ,  $\sum_{i=0}^w \binom{n+k}{i}$  candidates are generated, and the one that is optimal with respect to  $\delta$ -ADD is chosen as the output. As shown in Lemma 6, a new candidate can be generated from an error candidate by flipping a bit in the reliable subset and adding a certain vector to the unreliable subset. This corresponds to adding a logical operator in the normalizer group to the error candidate.

By examining these logical operators, we have the following degenerate error candidate pruning conditions.

**Theorem 8.** Consider an  $[[n, k, d]]$  stabilizer code with a check matrix given by  $[\mathbf{I}_{n-k} \ \mathbf{A}]$  after Gaussian elimination and a column permutation as in (5), where  $\mathbf{A} \in \{0, 1\}^{(n-k) \times (n+k)}$  are associated with the reliable bits of OSD<sub>4-0</sub> output.

- 1) When using  $n$ -ADD, only the reliable bits corresponding to nontrivial logical operators need to be considered in OSD<sub>4- $w$</sub> .
- 2) If each logical operator induced by flipping a reliable bit of OSD<sub>4-0</sub> output is a stabilizer, then OSD<sub>4- $w$</sub>  is equivalent to OSD<sub>4-0</sub> for any  $w$ .

*Proof.* 1) In  $n$ -ADD, different stabilizer cosets are compared. Therefore, multiplying a stabilizer by an error candidate does not create a new nontrivial candidate.

2) The statement is straightforward, as flipping these reliable bits results in only degenerate errors to the OSD<sub>4-0</sub> output.  $\square$

Exploiting Theorem 8-1) with  $n$ -ADD makes OSD<sub>4- $w$</sub>  more effective. By incorporating with the HRSR algorithm, we can work on a shortened check matrix  $\tilde{\mathbf{H}}$  and higher order of OSD can be executed. Consequently, (15) can be improved to  $w = \arg \max_x \sum_{i=0}^x \binom{u}{i} \leq \Gamma$ , where  $u \leq n+k-v+(m-m')$  is the number of columns in the shortened check matrix corresponding to nontrivial logical operators.

**Proposition 9.** Checking whether a logical operator induced by flipping a reliable bit of the OSD<sub>4-0</sub> output is a stabilizer can be done in  $O((n-k)k)$  time.

*Proof.* Consider an  $[[n, k, d]]$  stabilizer code with a  $m \times 2n$  check matrix  $\mathbf{H}$  and a  $2k \times 2n$  binary logical matrix  $\mathbf{L}$ . During the process of OSD<sub>4-0</sub>,  $\mathbf{H}$  leads to  $[\mathbf{I}_{n-k} \ \mathbf{A}]$  as in (5) using column permutations  $\pi, \mu$  and row operations  $R$ , where  $\mathbf{A} \in \{0, 1\}^{(n-k) \times (n+k)}$  are associated with the reliable bits of OSD<sub>4-0</sub> output.

By (11), flipping the  $j$ -th reliable bit corresponds to adding the vector  $\mathbf{g} = [\mathbf{A}_j^\top \ 0 \dots 0 \ 1 \ 0 \dots 0] \in \{0, 1\}^{2n}$ , where  $\mathbf{A}_j$  is the  $j$ -th column of  $\mathbf{A}$ . The vector  $\mathbf{g}$  corresponds to a stabilizer if  $\mu(\pi(\mathbf{L}\mathbf{A}))\mathbf{g}^\top = \mathbf{0}$ , and otherwise, it represents a nontrivial logical operator. Since  $\mathbf{A}_j$  is of dimension  $n - k$ , this computation takes  $O((n-k)k)$  time.  $\square$

The computational complexity of verifying such a bit-flipping event is  $O((n-k)k)$ , which implies that checking all the columns of  $A$  has a computational complexity of roughly the same order as Gaussian elimination. This approach is both effective and relatively efficient for implementing high-order OSD.

However, the complexity of  $n$ -ADD is not practically feasible. We may use  $\delta$ -ADD by choosing  $\delta$  as the highest weight of a set of low-weight stabilizer generators. For the case of a rotated surface code [25], the stabilizer generators are of weight 2 or 4, and the next lowest stabilizer weight is 6. Thus,  $n$ -ADD can be well approximated by 4-ADD at error rates lower than 1%. Assume that OSD<sub>4-0</sub> generates a list of error candidates  $\mathcal{E}$ . Then, 4-ADD outputs:

$$\hat{\mathbf{e}} = \arg \max_{\mathbf{e}} \sum_{i=0}^{n-k} \Pr \{ \mathbf{e} + \mathbf{H}_i \}, \quad (16)$$

where  $\mathbf{S}_0 = I$  and  $\{\mathbf{S}_i\}_{i=1}^{n-k}$  is a set of stabilizer generators for the rotated surface code. For practical implementation, let  $W(x)$  be the (Pauli) weight enumerator of the set  $\{\mathbf{E} + \mathbf{S}_i : i = 0, \dots, n-k\}$ , and then the calculation of (16) can be approximated by using the dominating terms in  $W(\epsilon/(1-\epsilon))$  for error rate  $\epsilon < 1\%$ .

For codes with algebraic structures, the first few lowest-weight terms can be derived, but determining the complete weight enumerator for a general code is an NP-hard problem. As an alternative, we propose selecting a set of  $m \geq n - k$  low-weight stabilizer generators and calculating the weight distribution of  $\binom{m}{c}$  stabilizers, where  $c$  is a constant independent of  $n$ . This method provides a good approximation of the dominant terms for practical purposes. To maintain an overall complexity of  $O(n^3)$ , the value of  $\binom{m}{c}$  should be chosen accordingly.

To achieve optimal execution complexity, 0-ADD is often used. Theorem 8 suggests focusing on the columns of  $A$  corresponding to nontrivial logical operators when  $n$ -ADD is used. However, in the scenario of 0-ADD, a stabilizer may influence the output of OSD<sub>4- $w$</sub>  since multiplying a stabilizer can reduce the weight of the error, potentially providing a better candidate in 0-ADD, even though the error coset

remains unchanged. Thus,  $\text{OSD}_{4-w}$  cannot simply flip bits corresponding to those nontrivial logical operators as in the case of Theorem 8-1).

However, Theorem 8-2) still works and we may use Proposition 9 to check this condition.

In the following we provide a weaker sufficient but operationally more efficient condition, for degenerate error candidate pruning.

**Corollary 10.** Let  $\tilde{S} \in \{0,1\}^{m' \times (2n-v)}$  be a shortened check matrix by the HRSR algorithm. Suppose that  $\tilde{S}$  can be transformed into  $[\mathbf{I} \ \tilde{\mathbf{A}}]$  after Gaussian elimination and a column permutation, where  $\tilde{\mathbf{A}}$  is associated with the reliable bits. If all the columns of  $\tilde{\mathbf{A}}$  are of weight less than  $d-1$ , then  $\text{OSD}_{4-w}$  on the corresponding reduced linear system is equivalent to  $\text{OSD}_{4-0}$  for any  $w$ .

The operational degenerate error pruning condition in Corollary 10 provides a more operationally efficient method to determine whether order- $w$  OSD for  $w > 0$  is nontrivial by evaluating the weight of each column. This can be done in  $O((n-k) \times (n+k))$ .

If there are many highly reliable bits, the number of stabilizers associated with these bits would be high. Consequently, the shortened check matrix  $\tilde{\mathbf{S}}$  from the HRSR algorithm will have fewer rows and lower column weights. Therefore, Corollary 10 can be applied with high probability when the error rate is low.

We combine all the aforementioned techniques into the approximate degenerate OSD (ADOSD) algorithm, as detailed in Algorithm 4, using 0-ADD. Note that if decoding performance is of higher priority,  $\delta$ -ADD can be utilized, and Proposition 9 can be integrated into Algorithm 4.

---

#### Algorithm 4 ADOSD<sub>4</sub>

---

**Input:** check matrix  $\mathbf{H} \in \{0,1\}^{m \times 2n}$  of rank  $n-k$ , syndrome  $\mathbf{s} \in \{0,1\}^{m \times 1}$ , BP output distributions  $\{\mathbf{q}_i\}_{i=1}^n$ , hard-decision reliability vector  $\boldsymbol{\eta} \in \mathbb{Z}^n$ , belief distributions  $\{\mathbf{q}_i\}_{i=1}^n$ , soft reliability threshold  $\theta$ , hard-decision vector  $\mathbf{e} \in \{0,1\}^{2n}$ , maximum number of OSD flips  $\Gamma$ , and backup OSD order  $w$ .  
**Output:** A valid error estimate  $\hat{\mathbf{e}} \in \{0,1\}^{2n}$ .

**Steps:**

Apply the HRSR algorithm.

**if** HRSR returns failure, **then**

use  $\text{OSD}_{4-w}$  to find an error estimate  $\hat{\mathbf{e}} \in \{0,1\}^{2n}$  for the original problem, and **return**  $\hat{\mathbf{e}}$ ;

**else** HRSR returns  $\mathbf{s}'$ ,  $\tilde{\mathbf{H}}$ ,  $\mathbf{e}^H$ , and  $\sigma$ .

**if** all the columns of  $\tilde{\mathbf{H}}$  in reduced row echelon form have weight less than  $d-1$ , **then**  $w \leftarrow 0$ ;

**else** determine  $w$  by (15).

**end if**

Use  $\text{OSD}_{4-w}$  on  $\mathbf{s}'$ ,  $\tilde{\mathbf{S}}$ , and the given data to find an error estimate  $\hat{\mathbf{e}}' \in \{0,1\}^{2n-v}$ , and **return**  $\sigma^{-1}([\hat{\mathbf{e}}' \ \mathbf{e}^H])$ .

**end if**

---

## VI. SIMULATION RESULTS

We simulate the performance of the MBP<sub>4</sub>+ADOSD<sub>4</sub> scheme on LCS codes [60], GHP codes [43], [44], BB

codes [56], and various 2D topological codes, including toric, rotated surface, color codes and twisted XZZX codes [23]–[27], [29], [59] (see [64, Table I]).

We use the MBP<sub>4</sub> decoder introduced in [32] as a predecoder for OSD. MBP<sub>4</sub> features a parameter  $\alpha$  that controls the step size of message updates during BP iterations: when  $\alpha < 1$ , the step size is enlarged; when  $\alpha > 1$ , the step size is reduced. For  $\alpha = 1$ , MBP<sub>4</sub> is equivalent to the refined BP<sub>4</sub> in [13]. We will specify the value of  $\alpha$  only when  $\alpha \neq 1$  is used. The optimization of  $\alpha$  is discussed in Section VI-A.

The maximum number of BP iterations,  $T$ , is set to 100 unless otherwise specified. Furthermore, our MBP<sub>4</sub>+ADOSD<sub>4</sub> scheme demonstrates robustness to variations in the maximum number of iterations, as discussed in Section VI-B. The soft reliability threshold is set to  $\theta = 0.999995$  and its selection is discussed in Section VI-C. In ADOSD<sub>4</sub> simulations,  $\Gamma$  is chosen according to (14) to enable comparison with OSD-2.

In Section VI-D, we compare the proposed BP+OSD schemes with various reliability measures using GHP codes. We then evaluate decoding performance on BB codes and topological codes in Sections VI-E, and VI-F. Finally, Section VI-G analyzes the execution time of these schemes, demonstrating the efficiency of ADOSD.

The decoding performance of a quantum code  $\mathcal{C}(\mathcal{S})$  and a decoder is assessed through the *logical error rate* (LER). For a code with distance  $d$ , errors up to  $t = \lfloor \frac{d-1}{2} \rfloor$  are correctable, while some errors of weight  $t+1$  become uncorrectable. Consequently, at low physical error rates, the performance curve of a decoder follows a scaling behavior of  $O(\epsilon^{t+1})$ . This implies that in a log-domain plot, the decoder's performance curve should exhibit an error floor with a slope of  $t+1$ . A good decoder will have a low error floor. However, if a decoder fails to correct all errors of weight up to  $t$ , the error floor will have a slope lower than  $t+1$ . In the worst case, a flatter error floor may appear earlier than expected.

Each data point in the plots is based on at least 100 logical error events in the low error rate regime. At LER  $10^{-6}$ , this represents an error bar less than  $2 \times 10^{-7}$ , which is roughly the size of the markers for the data points. Thus the error bars are neglected for clarity.

We observe that both parallel and serial schedules in MBP<sub>4</sub>+ADOSD<sub>4</sub> yield similar results for toric codes and surface codes. However, the parallel schedule outperforms the serial schedule on the [[882, 48, 16]] GHP code. We believe that this is because that the parallel schedule typically results in unsettled oscillations in BP, which can be resolved by OSD, whereas the serial schedule may make premature decisions on some bits, leading to incorrect convergence in the decoding process. Therefore, we consider the parallel schedule for the following simulations of MBP<sub>4</sub>+ADOSD<sub>4</sub>. Similar observations are also made in [55], [65].

For comparison, we consider several decoders listed in Table I. Except for AMBP, we do not implement these decoders ourselves but instead compare our results with those reported in the literature.

In [66], it was shown that a random order schedule improves BP decoding performance. Here, we implement the AMBP decoder with a random order serial schedule, achieving better

decoder	source	note
MBP <sub>4</sub> +ADOSD <sub>4</sub> MBP <sub>4</sub> +OSD <sub>4-w</sub> MBP <sub>4</sub> +mOSD <sub>4-w</sub>	this paper	based on Algorithm 4 reliability metric based on Definition 4 reliability metric based on Definition 5
AMBP <sub>4</sub>	[32]	No postprocessing. Can act as a predecoder for ADOSD <sub>4</sub> and OSD <sub>4</sub>
BP+mOSD(w,λ)	[43]	binary BP+ order-w OSD <sub>4</sub> with additional flips on λ positions
BP-OSD-CSλ	[44]	binary BP-OSD-0 with a greedy search on $\binom{3}{2}$ positions
BP+GDG	[55]	binary BP with guided decimation guessing based on a decision tree

TABLE I: Various decoders compared in this paper.

performance than the results reported in [32]. Note that AMBP incorporates various techniques for performance enhancement, and we do not focus on optimizing its performance in the following simulations.

#### A. Optimization of the parameter $\alpha$ in MBP<sub>4</sub> for ADOSD.

In this subsection, we demonstrate how to optimize the parameter  $\alpha$  of our MBP<sub>4</sub>+ADOSD<sub>4</sub> scheme using LCS codes [60] with  $T = 100$  and  $\theta = 0.999995$ . For most nondegenerate codes,  $\alpha = 1$  is sufficient to achieve good decoding performance. However, for degenerate codes, selecting  $\alpha > 1$  can result in more stable message passing, leading to improved OSD performance. This optimization should be conducted for each code and potentially for each error rate, though a single value of  $\alpha$  often applies across an entire code family.

LCS codes are a specialized type of quantum code that combines the features of surface codes and lift-product constructions. Decoding LCS codes presents the most challenging problem for AMBP<sub>4</sub> among all the quantum codes considered in this paper. We find that the AMBP<sub>4</sub> decoder [32] is ineffective for LCS codes, despite its superior performance over binary BP-OSD decoders [43], [44] on all other codes.

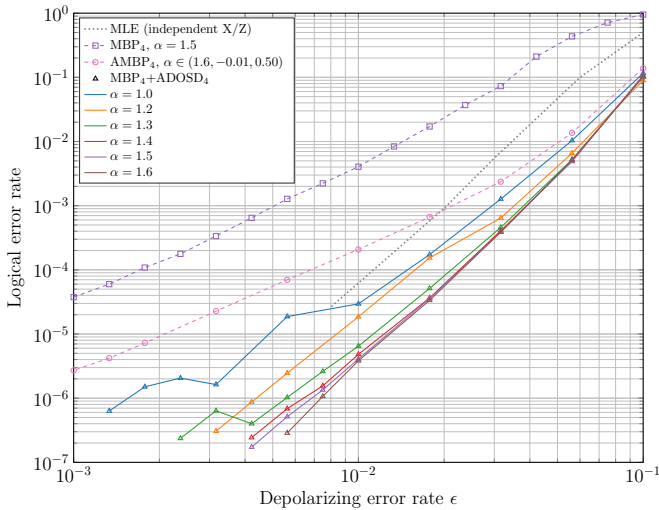


Fig. 2: MBP<sub>4</sub>+ADOSD<sub>4</sub> decoding with various values of  $\alpha$  for the  $[[175, 7, 7]]$  LCS code. The curve MLE is taken from [60]. The notation  $\alpha \in (1.6, -0.01, 0.50)$  means that  $\alpha$  is tested in the sequence 1.60, 1.59, 1.58, ..., 0.51, 0.50.

Figure 2 compares various decoders on the  $[[175, 7, 7]]$  LCS code, including an MLE (independent X/Z) reference curve from [60]. This MLE curve serves as a benchmark, as a decoder capable of correcting errors of weight up to 3 should exhibit a performance curve parallel to it at low error rates.

The performance of MBP<sub>4</sub>+ADOSD<sub>4</sub> on the  $[[175, 7, 7]]$  LCS code, with varying values of  $\alpha$ , exhibits fluctuations at lower values of  $\alpha$  but stabilizes as  $\alpha$  increases to 1.6. With  $\alpha = 1.6$ , its performance curve indicates that it can correct nearly all weight-3 errors at LER  $10^{-7}$ .

In [60], the BP-OSD-CS60 decoder was shown to closely match the MLE curve on this code. Since the decoding of  $X$  and  $Z$  errors is performed independently, the MLE curve represents optimal performance under the assumption that  $X$  and  $Z$  errors are uncorrelated. As MBP<sub>4</sub>+ADOSD<sub>4</sub> leverages the  $X/Z$  correlations, it significantly outperforms both the MLE curve and BP-OSD-CS60 by more than 15 times. In contrast, AMBP<sub>4</sub> encounters an error floor for  $\epsilon \leq 0.03$ .

We observe a similar performance of MBP<sub>4</sub>+ADOSD<sub>4</sub> for  $[[15, 3, 3]]$ ,  $[[65, 5, 5]]$  and  $[[369, 9, 9]]$  LCS codes as well, while AMBP has an even higher error floor around LER  $10^{-2}$  for the  $[[369, 9, 9]]$  LCS code and a lower error floor around  $10^{-5}$  for the  $[[65, 5, 5]]$  LCS code.

For improved performance,  $\alpha$  can be adaptively chosen for each  $\epsilon$ , as demonstrated in Section VI-D.

#### B. Robustness of the maximum iterations in MBP<sub>4</sub>+ADOSD<sub>4</sub>

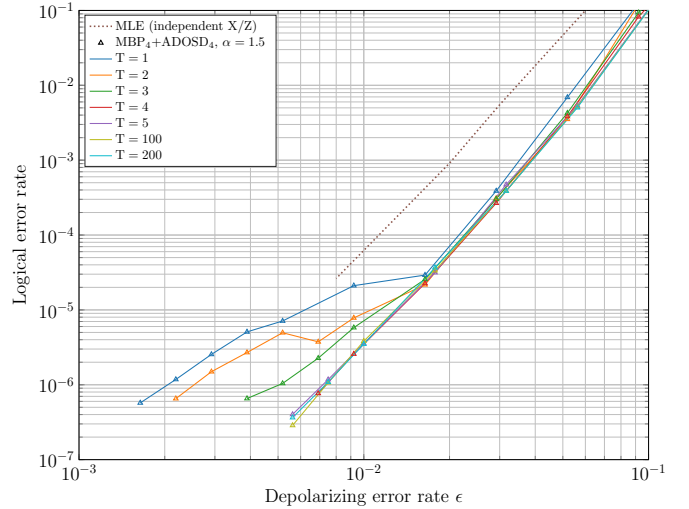


Fig. 3: MBP<sub>4</sub>+ADOSD<sub>4</sub> decoding with various maximum number of iterations  $T$  for the  $[[175, 7, 7]]$  LCS code.

Next, we demonstrate that the performance of ADOSD<sub>4</sub> remains robust even with variations in the maximum number of iterations in MBP<sub>4</sub>. We note that in ADOSD<sub>4</sub>, OSD- $w$  is invoked when HRSR fails. As a result, the overall algorithm maintains high accuracy. However, the failures of the HRSR algorithm can impact the simulation time, as OSD- $w$  is significantly more time-consuming.

Figure 3 illustrates the performance of MBP<sub>4</sub>+ADOSD<sub>4</sub> decoding for the  $[[175, 7, 7]]$  LCS code with varying maximum numbers of iterations,  $T = 1, 2, 3, 4, 5, 100, 200$ . The curve

$\epsilon$	0.1	0.056	0.032	0.018	0.01	0.007	0.0056
Avg. iter.	194.46	97.67	23.51	6.31	2.44	1.70	1.23

TABLE II: The average number of iterations for MBP<sub>4</sub> decoding on the  $[[175, 7, 7]]$  LCS code with  $T = 200$ .

for  $T = 4$  is already good enough and smooth. While increasing the number of iterations results in slightly improved performance, the curves converge closely around an LER of  $2 \times 10^{-7}$  to  $3 \times 10^{-7}$ .

Table II presents the average number of iterations for  $T = 200$ . It can be observed that the average number of iterations rapidly decreases to one or two when  $\epsilon < 0.01$ . Since we are targeting lower error rates, to balance accuracy and efficiency, we typically choose  $T = 100$ .

### C. Selection of Reliability Threshold

We now discuss the selection of the reliability threshold. Figure 4 presents an example for the  $[[175, 7, 7]]$  LCS code, which is representative of our simulation results.

Based on our experience, at high error rates, the reliability threshold has little impact on performance. However, at low error rates, where higher accuracy is required, the choice of  $\theta$  depends on both  $T$  and the specific code. For instance, MBP<sub>4</sub>+ADOSD<sub>4</sub> achieves excellent performance on the  $[[175, 7, 7]]$  LCS code with  $T = 2$  and  $\theta = 0.5$  but performs poorly on the (4.8.8) color code with  $d = 5$  under the same setting.

With  $T = 100$  and  $\theta = 0.999995$ , we generally observe good and stable decoding performance across all codes considered, as shown in Figure 4. Therefore, we adopt these values for our analysis in the following subsections.

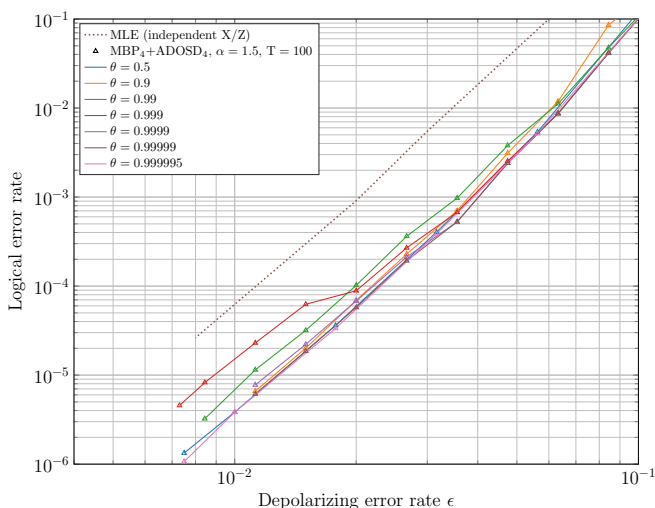


Fig. 4: MBP<sub>4</sub>+ADOSD<sub>4</sub> decoding with various values of reliability threshold  $\theta$  for the  $[[175, 7, 7]]$  LCS code.

### D. Generalized hypergraph-product codes

The  $[[882, 48, 16]]$  GHP code [43] is highly degenerate, which causes conventional BP to perform poorly. Figure 5 presents the performance curves of different MBP and OSD

combinations, where  $\alpha$  is either fixed at 1.6 or adaptively chosen as  $\alpha(\epsilon)$ .

For comparison, we also include the performance of AMBP<sub>4</sub> [32] and BP+mOSD( $w, \lambda$ ) [43]. BP+mOSD( $w, \lambda$ ) exhibits an early error floor around  $\epsilon = 0.09$ . Both MBP<sub>4</sub>+ADOSD<sub>4</sub> and MBP<sub>4</sub>+OSD<sub>4</sub>-2 with  $\alpha = 1.6$  outperform BP+mOSD(15, 15) [43] by more than an order of magnitude at  $\epsilon = 0.05$ .

It was suggested in [32, Fig.3] (arXiv version) that  $\alpha$  and  $\epsilon$  follow the relationship  $\alpha(\epsilon) = -0.16 \log_{10}(\epsilon) - 0.48$ , with the coefficients  $-0.16$  and  $-0.48$  determined through pre-simulations on the  $[[882, 48]]$  code. From Figure 5, MBP<sub>4</sub>+ADOSD<sub>4</sub>( $\alpha(\epsilon)$ ) improves upon MBP<sub>4</sub>+ADOSD<sub>4</sub> with a fixed  $\alpha = 1.6$ , particularly at high error rates. Additionally, MBP<sub>4</sub>+ADOSD<sub>4</sub>( $\alpha(\epsilon)$ ) performs slightly better than MBP<sub>4</sub>+OSD<sub>4</sub>-2( $\alpha(\epsilon)$ ).

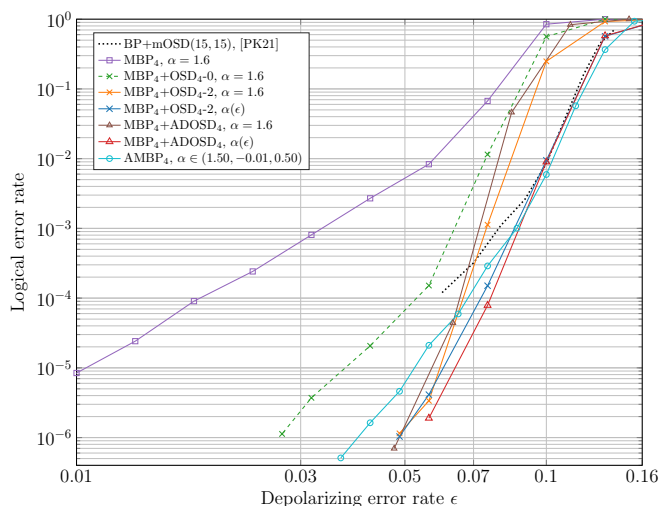


Fig. 5: Comparison of various decoders on the  $[[882, 48, 16]]$  GHP code. The curve BP+mOSD(15,15) is from [43].

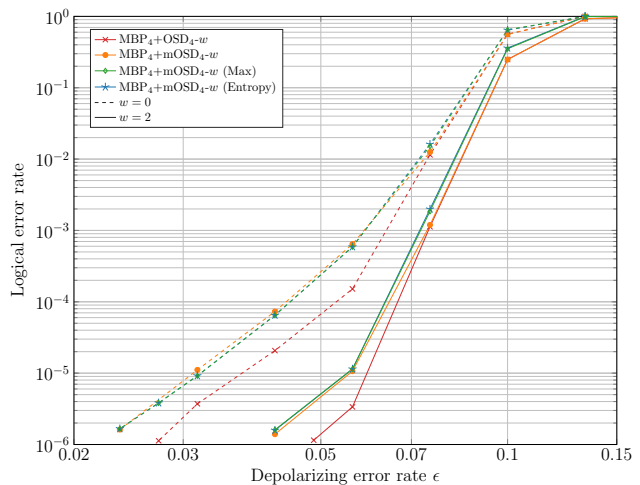


Fig. 6: Comparison of various metrics for reliability order in MBP<sub>4</sub>-OSD<sub>4</sub> on the  $[[882, 48, 16]]$  GHP code with  $\alpha = 1.6$ .

In ADOSD<sub>4</sub>, we propose using integrated hard-decision and soft reliabilities as a reliability metric (Definition 4). Herein

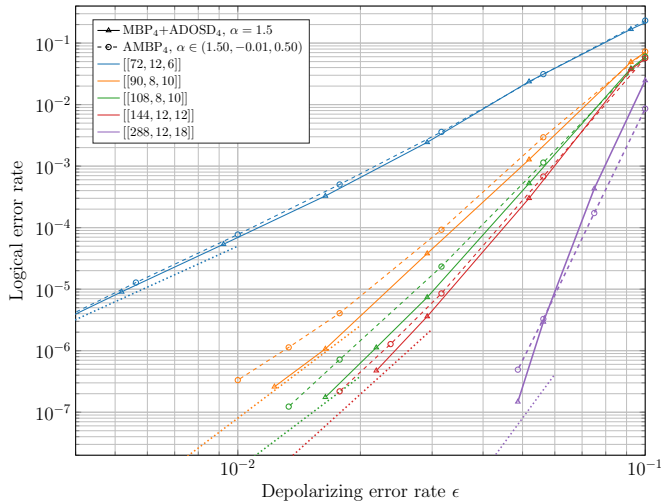


Fig. 7:  $\text{MBP}_4$  and  $\text{MBP}_4+\text{ADOSD}_4$  decoding performance for various BB codes.

we also simulate the performances of  $\text{MBP}_4+\text{mOSD}$  based on the reliability metrics of Entropy or Max as shown in Figure 6, including  $\text{mOSD}_4$  as well. Two conclusions are as follows:

- 1) The reliability metric in Definition 4, which incorporates historical message information, outperforms other metrics that rely solely on the last belief distributions.
- 2) The performances of  $\text{mOSD}$  based on Definition 5, Entropy, or Max are mostly comparable;  $\text{mOSD}-w$  based on Definition 5 is slightly better than the other two metrics at lower error rate for  $w = 2$ .

### E. Bivariate bicycle codes

BB codes are a class of QLDPC codes proposed in [56], featuring a high error threshold and a significantly higher code rate than topological codes. Several attempts at decoding this code family have been presented in [54], [55] under the code capacity noise model. However, the BP+CB decoder in [54] does not perform as well as BP-OSD-0. The BP+GDG decoder in [55] shows improved performance, surpassing BP-OSD-0 and being comparable to BP2-OSD-CS10 over independent X errors, as shown in [55, Figure 4].

Figure 7 presents the simulation results of  $\text{MBP}_4+\text{ADOSD}_4$  and  $\text{AMBP}_4$  decoding for BB codes, both of which demonstrate significantly better performance than GDG decoding. For instance, consider the  $[[144, 12, 12]]$  BB code. At an  $X$  error rate of 0.02 (corresponding to a depolarizing rate of about 0.03), BP+GDG achieves an LER of approximately  $10^{-4}$ . In contrast, both  $\text{MBP}_4+\text{ADOSD}_4$  and  $\text{AMBP}_4$  achieve an LER below  $4 \times 10^{-6}$  at the same depolarizing rate. Moreover,  $\text{MBP}_4+\text{ADOSD}_4$  outperforms  $\text{AMBP}_4$ .

For reference, we include dotted  $O(\epsilon^{t+1})$  curves for each code. The  $[[72, 12, 6]]$  and  $[[90, 8, 10]]$  codes closely follow these reference curves, while the other three codes exhibit lower error floors below LER  $10^{-7}$ .

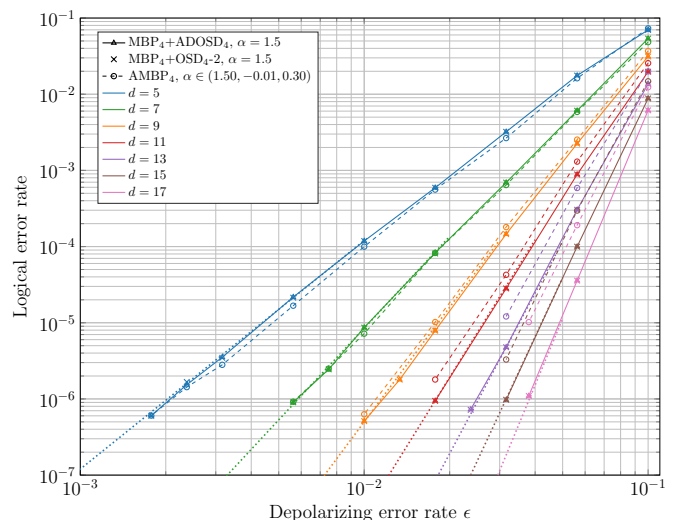


Fig. 8:  $\text{MBP}_4+\text{OSD}_4-2$ ,  $\text{MBP}_4+\text{ADOSD}_4$ , and  $\text{AMBP}_4$  decoding performance for various  $[[d^2, 1, d]]$  rotated surface codes.

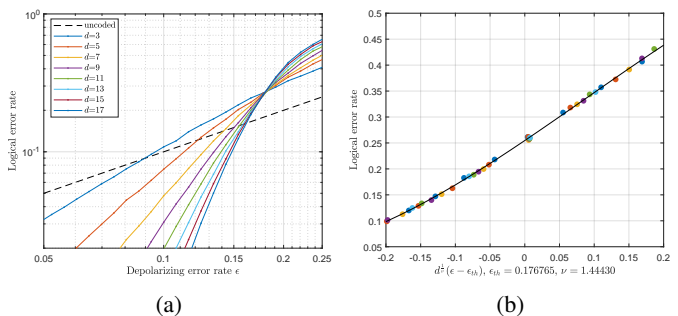


Fig. 9: (a) The threshold of  $\text{MBP}_4+\text{OSD}_4-2$  on the  $[[d^2, 1, d]]$  rotated surface codes with  $\alpha = 1.0$  is about 17.67% from the simulations. For each data point, we collected at least 10,000 logical error events. The dashed line stands for no error correction. (b) The accuracy of the threshold estimation about  $\text{MBP}_4+\text{OSD}_4-2$  on the rotated surface codes can be demonstrated using the critical scaling approach. The estimation is based on data from  $d = 7$  to  $d = 17$ , ensuring that the results are not influenced by biased information.

### F. 2D topological codes

Here, we evaluate the decoding performance of our BP+OSD schemes on various 2D topological codes. Examining LER around  $10^{-6}$  is important, as it helps identify whether an iterative decoder exhibits error floor behavior.

Figure 8 presents the performance curves of  $\text{MBP}_4+\text{ADOSD}_4$  and  $\text{MBP}_4+\text{OSD}_4-2$  on  $[[d^2, 1, d]]$  rotated surface codes with distances ranging from 5 to 17. They exhibit excellent performance, closely following the dotted reference curves.

The threshold analysis for  $[[d^2, 1, d]]$  rotated surface codes, conducted using the scaling ansatz method [67], [68], is shown in Figure 9. The results show a threshold of approximately 17.67% for BP+OSD-2, with  $\text{MBP}_4+\text{ADOSD}_4$  exhibiting nearly identical performance. Notably, they outperform  $\text{AMBP}_4$ , particularly for larger  $d$ , resulting in a higher

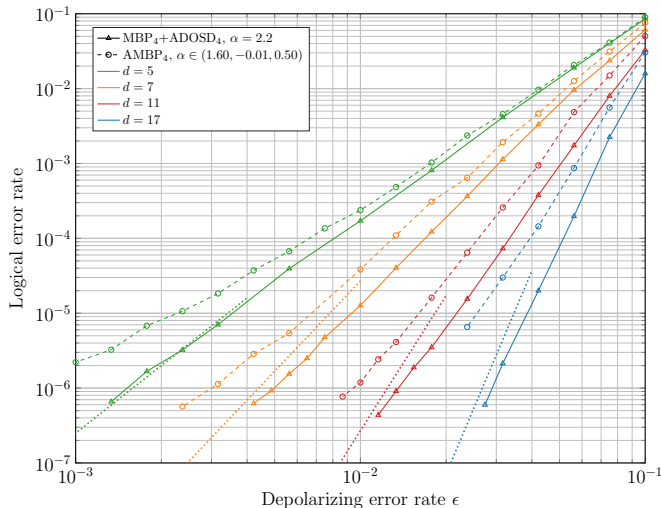


Fig. 10: AMBP<sub>4</sub> and MBP<sub>4</sub>+ADOSD<sub>4</sub> decoding performance for various (4.8.8) color codes.

TABLE III: Thresholds for 2D topological codes subject to depolarizing errors. The parameter for MBP<sub>4</sub> is set to  $\alpha = 1.0$ .

code family	MBP <sub>4</sub> +OSD <sub>4-2</sub>	MBP <sub>4</sub> +ADOSD <sub>4</sub>	AMBP <sub>4</sub>
rotated toric	17.52%	17.52%	≈ 17.5%
rotated surface	17.67%	17.67%	≈ 16%
(6.6.6) color	15.41%	15.18%	≈ 14.5%
(4.8.8) color	15.09%	14.69%	≈ 14.5%
XZZX twisted	17.72%	17.72%	≈ 17.5%

threshold compared to the 16% threshold of AMBP<sub>4</sub>.

In summary, our decoding schemes demonstrate superior performance on surface codes compared to the MWPM decoder [69], [70], both in terms of LER performance and error threshold (see, e.g., [71]).

Similar analyses are performed for toric, twisted XZZX, (6.6.6), and (4.8.8) color codes using both BP<sub>4</sub>+OSD<sub>4-2</sub> and BP<sub>4</sub>+ADOSD<sub>4</sub>. The summarized threshold results are presented in Table III. ADOSD<sub>4</sub> and OSD<sub>4-2</sub> exhibit nearly identical performances on toric, surface, and twisted XZZX codes, with OSD<sub>4-2</sub> performing slightly better on the (6.6.6) and (4.8.8) color codes.

The thresholds for the color codes are lower than those of toric and surface codes. This is evident from the performance curves of the (4.8.8) color codes as shown in Figure 10. While the slopes of these curves increase as the error rate decreases, they do not closely match the slopes of the dotted reference curves. This suggests that some low-weight errors, even those with weight less than  $t + 1$ , may remain uncorrected by these decoders. Consequently, additional techniques or higher-order OSD may be necessary.

### G. Time consumption

In the previous subsections, we have demonstrated the effectiveness of our BP+OSD schemes. In this subsection we analyze the time efficiency of our OSD schemes. We fix  $\alpha = 1$  in MBP<sub>4</sub>.

#### 1) Time Consumption of ADOSD<sub>4</sub> vs. OSD<sub>4-2</sub> and BP:

Table IV lists the average time consumptions of MBP<sub>4</sub>, ADOSD<sub>4</sub>, and OSD<sub>4-2</sub> for surface codes with distances of 11, 13, and 15 at LER around  $10^{-6}$ . The unit of time is microseconds ( $\mu$ s) measured using a single-thread desktop computer. To achieve LER  $10^{-6}$  using MBP<sub>4</sub>+ADOSD<sub>4</sub>, the physical error rates are set to 0.017, 0.025, and 0.033 for codes with distances 11, 13, and 15, respectively. At least  $10^5$  samples are collected for each case.

It can be observed that the time consumption of ADOSD<sub>4</sub> is approximately 2% to 4% of that of OSD<sub>4-2</sub>, with similar results observed for other quantum codes in this study. In summary, ADOSD<sub>4</sub> is at least 25 times faster than OSD<sub>4-2</sub> at an LER of around  $10^{-6}$ .

Table IV also lists the time consumption of ADOSD<sub>4</sub> in terms of MBP<sub>4</sub> iterations. Specifically, the average time consumption per codeword for ADOSD<sub>4</sub> is approximately equivalent to 1.76 to 2.21 MBP<sub>4</sub> iterations. This shows that the time consumption for ADOSD<sub>4</sub> is roughly equivalent to 1 to 2 successful MBP<sub>4</sub> executions.

2) *HRSR and OSD-0 in ADOSD<sub>4</sub>*: We have shown that ADOSD<sub>4</sub> is efficient, thanks to Algorithm 3 and Corollary 10. These methods reduce the effective length using reliable subset reduction and allow us to perform only OSD<sub>4-0</sub> by identifying degenerate error cosets. Now, we examine the effectiveness of these techniques on the surface code of distance 11, with similar results observed for distances 13 and 15.

Table V enumerates the percentage of ADOSD<sub>4</sub> trials that only perform OSD<sub>4-0</sub> using Corollary 10. At  $\epsilon = 4.1\%$ , 93.61% of ADOSD<sub>4</sub> trials already perform only OSD<sub>4-0</sub>, increasing to 99.84% at  $\epsilon = 1.7\%$ . Thus, at lower error rates, almost all trials execute OSD<sub>4-0</sub>.

Moreover, the HRSR algorithm reduces the dimensions of the check matrix in both rows and columns. Table V also provides the percentages of trials where the number of rows and columns in the check matrix is reduced to 20% or 30% of the original (denoted as 20% and 30% effective dimensions in the table). These percentages increase quickly as the error rate decreases. With fewer than 30% effective dimensions, the time consumption for Gaussian elimination reduces to roughly  $0.3^3 = 2.7\%$ , consistent with the previous results.

## VII. CONCLUSION

We proposed quaternary OSD with integrated hard- and soft-decision reliabilities to retain the  $X/Z$  correlations. Our BP-OSD schemes have demonstrated highly effective decoding capabilities for various sparse quantum codes in the code capacity noise model, including both CSS and non-CSS codes. Additionally, when the logical error rate is around  $10^{-6}$ , ADOSD<sub>4</sub> can further enhance the decoding process by offering accelerated decoding while maintaining comparable performance. As a result, ADOSD<sub>4</sub> is applicable to small or medium-sized codes with  $n \approx 1000$ , significantly enhancing the performance of BP in the code capacity noise model. In our simulations, we restricted the number of error candidates to the size of order-2 OSD; better performance of ADOSD<sub>4</sub> can be achieved by allowing for greater options.

TABLE IV: Comparison of the time consumption for surface codes at LER about  $10^{-6}$ .

code distance	$\epsilon$	MBP <sub>4</sub> failure rate	time per MBP <sub>4</sub> iteration ( $\mu$ s)	time per ADOSD <sub>4</sub> ( $\mu$ s)	time per OSD <sub>4-2</sub> ( $\mu$ s)	average iterations when MBP <sub>4</sub> succeeds	ADOSD <sub>4</sub> time <sup>†</sup> in MBP <sub>4</sub> iterations
11	1.7%	21.46%	0.01464	0.0272	0.667	1.002	2
13	2.5%	35.97%	0.0212	0.0469	1.342	1.79	2.21
15	3.3%	51.47%	0.0287	0.0506	2.155	2.41	1.76

<sup>†</sup> : the time per ADOSD<sub>4</sub> operation divided by the time per MBP<sub>4</sub> iteration.

TABLE V: Percentage of OSD-0 in ADOSD<sub>4</sub> on the surface code of distance 11

depolarizing rate $\epsilon$	1.7%	2.7%	4.1%
LER	$10^{-6}$	$10^{-5}$	$10^{-4}$
OSD-0	99.84%	98.85%	93.61%
20% effective dimensions	44.13%	26.30%	5.13%
30% effective dimensions	94.04%	84.46%	57.91%

We note that while all the techniques developed in this paper are presented in the context of quaternary error variables, they can naturally be adapted to binary OSD for handling CSS codes. This includes hard-decision reliability, highly reliable subset reduction, approximate degenerate decoding, and degenerate candidate pruning conditions, by restricting the approach to either  $X$ - or  $Z$ -stabilizers. Furthermore, these techniques can be integrated with other methods available in the literature.

In our investigations, we primarily focused on MBP<sub>4</sub>+OSD<sub>4-2</sub> and ADOSD<sub>4</sub>. However, MBP<sub>4</sub>+OSD<sub>4-0</sub> has also exhibited excellent performance for most codes, aligning with the findings in [43]. In particular, we found that ADOSD<sub>4</sub> mostly performs only MBP<sub>4</sub>+OSD<sub>4-0</sub> at low error rates. On the other hand, at low error rates (e.g., below  $10^{-3}$ ), there are small non-isolated errors, so the effective length for OSD is relatively small, allowing us to perform higher-order OSD. We have observed some instances of surface codes with order  $w$  up to 13 in (14).

An interesting observation is that we can identify bit-flips in error candidates corresponding to multiplying a stabilizer operator, as stated in Theorem 8 and Corollary 10. This information can be used to improve the algorithm by flipping effective bits in approximate degenerate decoding. Additionally, another potential improvement is extending the candidate pruning condition by Fossorier *et al.* [47] to quantum codes.

We chose the binary representation of quantum codes and syndrome correction for developing the OSD algorithm. A quantum code can be interpreted as a quaternary additive code with binary error syndromes [6]. Thus, one might consider formulating a system consisting of  $n$  quaternary variables and  $n - k$  additive constraints and employ a Gaussian elimination process for quaternary additive groups. However, for practical implementation, we chose to binarize this process.

There are various reliability metrics that consider the (weighted) accumulation of the log-likelihood ratio (LLR) signs for each bit during BP iterations [72]–[75]. Our hard-decision reliability can be viewed as an extension of this idea, focusing on the length of the last run in the hard-decision

vectors. The reliability order in Definition 4 can be adapted to employ alternative metrics, such as Entropy or Max [43]. From our experiments, the integrated hard- and soft-decision reliabilities yielded the best results.

Finally, there is significant progress in circuit-level error decoding [56], [76]–[79]. Various decoders have been shown to work for circuit-level noise models, including BP-OSD-CS, GDG, ambiguity clustering [57], LSD [58], and ordered Tanner forest [80]. Our BP-OSD scheme can be extended to handle both data and syndrome errors in the phenomenological noise model [81], [82], using techniques proposed in [83]–[85], as demonstrated in our recent work [86].

## REFERENCES

- [1] C.-F. Kung, K.-Y. Kuo, and C.-Y. Lai, "On belief propagation decoding of quantum codes with quaternary reliability statistics," in *2023 12th International Symposium on Topics in Coding (ITC)*, 2023, pp. 1–5.
- [2] D. Gottesman, "Fault-tolerant quantum computation with constant overhead," *Quantum Info. Comput.*, vol. 14, no. 15&16, pp. 1338–1372, Nov. 2014.
- [3] B. M. Terhal, "Quantum error correction for quantum memories," *Reviews of Modern Physics*, vol. 87, no. 2, pp. 307–346, 2015.
- [4] C.-Y. Lai and K.-Y. Kuo, "Harnessing coding theory for reliable network quantum communication," *IEEE Wireless Communications*, vol. 31, no. 4, pp. 82–88, 2024.
- [5] D. Gottesman, "Stabilizer codes and quantum error correction," Ph.D. dissertation, Caltech, 1997.
- [6] A. R. Calderbank, E. M. Rains, P. W. Shor, and N. J. A. Sloane, "Quantum error correction via codes over GF(4)," *IEEE Trans. Inf. Theory*, vol. 44, no. 4, pp. 1369–1387, 1998.
- [7] M. A. Nielsen and I. L. Chuang, *Quantum Computation and Quantum Information*. Cambridge University Press, 2000.
- [8] D. J. C. MacKay, G. Mitchison, and P. L. McFadden, "Sparse-graph codes for quantum error correction," *IEEE Trans. Inf. Theory*, vol. 50, no. 10, pp. 2315–2330, 2004.
- [9] D. Poulin and Y. Chung, "On the iterative decoding of sparse quantum codes," *Quantum Inf. Comput.*, vol. 8, pp. 987–1000, 2008.
- [10] Y.-J. Wang, B. C. Sanders, B.-M. Bai, and X.-M. Wang, "Enhanced feedback iterative decoding of sparse quantum codes," *IEEE Trans. Inf. Theory*, vol. 58, no. 2, pp. 1231–1241, 2012.
- [11] Z. Babar, P. Botsinis, D. Alanis, S. X. Ng, and L. Hanzo, "Fifteen years of quantum LDPC coding and improved decoding strategies," *IEEE Access*, vol. 3, pp. 2492–2519, 2015.
- [12] A. Rigby, J. C. Olivier, and P. Jarvis, "Modified belief propagation decoders for quantum low-density parity-check codes," *Phys. Rev. A*, vol. 100, no. 1, p. 012330, 2019.
- [13] K.-Y. Kuo and C.-Y. Lai, "Refined belief propagation decoding of sparse-graph quantum codes," *IEEE J. Sel. Areas Inf. Theory*, vol. 1, no. 2, pp. 487–498, 2020.
- [14] C.-Y. Lai and K.-Y. Kuo, "Log-domain decoding of quantum LDPC codes over binary finite fields," *IEEE Trans. Quantum Eng.*, vol. 2, 2021, article no. 2103615.
- [15] R. G. Gallager, "Low-density parity-check codes," *IRE Trans. Inf. Theory*, vol. 8, no. 1, pp. 21–28, 1962.
- [16] D. J. C. MacKay and R. M. Neal, "Good codes based on very sparse matrices," in *Proc. IMA Int. Conf. Cryptogr. Coding*, 1995, pp. 100–111.
- [17] D. MacKay, "Good error-correcting codes based on very sparse matrices," *IEEE Trans. Inf. Theory*, vol. 45, no. 2, pp. 399–431, 1999.
- [18] R. Tanner, "A recursive approach to low complexity codes," *IEEE Trans. Inf. Theory*, vol. 27, no. 5, pp. 533–547, 1981.

- [19] J. Pearl, *Probabilistic reasoning in intelligent systems: networks of plausible inference*. Kaufmann, 1988.
- [20] F. R. Kschischang, B. J. Frey, and H.-A. Loeliger, "Factor graphs and the sum-product algorithm," *IEEE Trans. Inf. Theory*, vol. 47, no. 2, pp. 498–519, 2001.
- [21] A. R. Calderbank and P. W. Shor, "Good quantum error-correcting codes exist," *Phys. Rev. A*, vol. 54, p. 1098, 1996.
- [22] A. M. Steane, "Error correcting codes in quantum theory," *Phys. Rev. Lett.*, vol. 77, p. 793, 1996.
- [23] A. Y. Kitaev, "Fault-tolerant quantum computation by anyons," *Annals of Physics*, vol. 303, no. 1, pp. 2–30, 2003.
- [24] H. Bombin and M. A. Martin-Delgado, "Topological quantum distillation," *Phys. Rev. Lett.*, vol. 97, no. 18, p. 180501, 2006.
- [25] H. Bombin and M. A. Martin-Delgado, "Optimal resources for topological two-dimensional stabilizer codes: Comparative study," *Phys. Rev. A*, vol. 76, no. 1, p. 012305, 2007.
- [26] C. Horsman, A. G. Fowler, S. Devitt, and R. Van Meter, "Surface code quantum computing by lattice surgery," *New J. Phys.*, vol. 14, no. 12, p. 123011, 2012.
- [27] B. Terhal, F. Hassler, and D. DiVincenzo, "From Majorana fermions to topological order," *Phys. Rev. Lett.*, vol. 108, no. 26, p. 260504, 2012.
- [28] A. J. Landahl, J. T. Anderson, and P. R. Rice, "Fault-tolerant quantum computing with color codes," *arXiv preprint arXiv:1108.5738*, 2011.
- [29] J. Bonilla Ataides, D. Tuckett, S. Bartlett, S. Flammia, and B. Brown, "The XZZX surface code," *Nat. Commun.*, vol. 12, no. 1, pp. 1–12, 2021.
- [30] N. Raveendran and B. Vasić, "Trapping sets of quantum LDPC codes," *Quantum*, vol. 5, p. 562, 2021.
- [31] D. Chytas, M. Pacenti, N. Raveendran, M. F. Flanagan, and B. Vasić, "Enhanced message-passing decoding of degenerate quantum codes utilizing trapping set dynamics," *IEEE Communications Letters*, vol. 28, no. 3, pp. 444–448, 2024.
- [32] K.-Y. Kuo and C.-Y. Lai, "Exploiting degeneracy in belief propagation decoding of quantum codes," *npj Quantum Inf.*, vol. 8, 2022, article no. 111. [Online]. Available: <https://arxiv.org/abs/2104.13659>
- [33] M. P. Fossorier and S. Lin, "Soft-decision decoding of linear block codes based on ordered statistics," *IEEE Trans. Inf. Theory*, vol. 41, no. 5, pp. 1379–1396, 1995.
- [34] J. Wolf, "Efficient maximum likelihood decoding of linear block codes using a trellis," *IEEE Trans. Inf. Theory*, vol. 24, no. 1, pp. 76–80, 1978.
- [35] A. Lafourcade and A. Vardy, "Asymptotically good codes have infinite trellis complexity," *IEEE Trans. Inf. Theory*, vol. 41, no. 2, pp. 555–559, 1995.
- [36] P. Elias, "List decoding for noisy channels," in *IRE WESCON Conv. Rec.*, 1957, pp. 94–104.
- [37] —, "Error-correcting codes for list decoding," *IEEE Trans. Inf. Theory*, vol. 37, no. 1, pp. 5–12, 1991.
- [38] G. Forney, "Generalized minimum distance decoding," *IEEE Trans. Inf. Theory*, vol. 12, no. 2, pp. 125–131, 1966.
- [39] D. Chase, "Class of algorithms for decoding block codes with channel measurement information," *IEEE Trans. Inf. Theory*, vol. 18, no. 1, pp. 170–182, 1972.
- [40] J. Snyders and Y. Be'erly, "Maximum likelihood soft decoding of binary block codes and decoders for the Golay codes," *IEEE Trans. Inf. Theory*, vol. 35, no. 5, pp. 963–975, 1989.
- [41] T. Kaneko, T. Nishijima, H. Inazumi, and S. Hirasawa, "An efficient maximum-likelihood-decoding algorithm for linear block codes with algebraic decoder," *IEEE Trans. Inf. Theory*, vol. 40, no. 2, pp. 320–327, 1994.
- [42] Y. S. Han, C. R. Hartmann, and C.-C. Chen, "Efficient priority-first search maximum-likelihood soft-decision decoding of linear block codes," *IEEE Trans. Inf. Theory*, vol. 39, no. 5, pp. 1514–1523, 1993.
- [43] P. Pantelev and G. Kalachev, "Degenerate quantum LDPC codes with good finite length performance," *Quantum*, vol. 5, p. 585, 2021. [Online]. Available: <https://arxiv.org/abs/1904.02703>
- [44] J. Roffe, D. R. White, S. Burton, and E. Campbell, "Decoding across the quantum low-density parity-check code landscape," *Phys. Rev. Res.*, vol. 2, no. 4, p. 043423, 2020.
- [45] M. Fossorier, "Iterative reliability-based decoding of low-density parity check codes," *IEEE Journal on Selected Areas in Communications*, vol. 19, no. 5, pp. 908–917, 2001.
- [46] M. Baldi, F. Chiaraluce, N. Maturo, G. Liva, and E. Paolini, "A hybrid decoding scheme for short non-binary LDPC codes," *IEEE Communications Letters*, vol. 18, no. 12, pp. 2093–2096, 2014.
- [47] M. P. Fossorier, S. Lin, and J. Snyders, "Reliability-based syndrome decoding of linear block codes," *IEEE Trans. Inf. Theory*, vol. 44, no. 1, pp. 388–398, 1998.
- [48] M. P. Fossorier and S. Lin, "Computationally efficient soft-decision decoding of linear block codes based on ordered statistics," *IEEE Trans. Inf. Theory*, vol. 42, no. 3, pp. 738–750, 1996.
- [49] D. Gazelle and J. Snyders, "Reliability-based code-search algorithms for maximum-likelihood decoding of block codes," *IEEE Trans. Inf. Theory*, vol. 43, no. 1, pp. 239–249, 1997.
- [50] S. E. Alnawayseh and P. Loskot, "Ordered statistics-based list decoding techniques for linear binary block codes," *EURASIP J. Wireless Commun. Netw.*, vol. 2012, pp. 1–12, 2012.
- [51] C. Yue, M. Shirvanimoghaddam, Y. Li, and B. Vucetic, "Segmentation-discarding ordered-statistic decoding for linear block codes," in *IEEE Global Commun. Conf. (GLOBECOM)*, 2019, pp. 1–6.
- [52] C. Yue, M. Shirvanimoghaddam, B. Vucetic, and Y. Li, "A revisit to ordered statistics decoding: Distance distribution and decoding rules," *IEEE Trans. Inf. Theory*, vol. 67, no. 7, pp. 4288–4337, 2021.
- [53] L. Yang, W. Chen, and L. Chen, "Reduced complexity ordered statistics decoding of linear block codes," in *2022 IEEE/CIC International Conference on Communications in China (ICC Workshops)*, 2022, pp. 371–376.
- [54] A. d. iOlus and J. E. Martínez, "The closed-branch decoder for quantum ldpc codes," *arXiv preprint arXiv:2402.01532*, 2024.
- [55] A. Gong, S. Cammerer, and J. M. Renes, "Toward low-latency iterative decoding of qldpc codes under circuit-level noise," *arXiv preprint arXiv:2403.18901*, 2024.
- [56] S. Bravyi, A. W. Cross, J. M. Gambetta, D. Maslov, P. Rall, and T. J. Yoder, "High-threshold and low-overhead fault-tolerant quantum memory," *Nature*, vol. 627, no. 8005, pp. 778–782, 2024.
- [57] S. Wolanski and B. Barber, "Ambiguity clustering: an accurate and efficient decoder for QLDPC codes," *arXiv preprint arXiv:2406.14527*, 2024.
- [58] T. Hillmann, L. Berent, A. O. Quintavalle, J. Eisert, R. Wille, and J. Roffe, "Localized statistics decoding: A parallel decoding algorithm for quantum low-density parity-check codes," *arXiv preprint arXiv:2406.18655*, 2024.
- [59] A. A. Kovalev, I. Dumer, and L. P. Pryadko, "Design of additive quantum codes via the code-word-stabilized framework," *Phys. Rev. A*, vol. 84, no. 6, p. 062319, 2011.
- [60] J. Old, M. Rispler, and M. Müller, "Lift-connected surface codes," *Quantum Science and Technology*, vol. 9, no. 4, p. 045012, jul 2024. [Online]. Available: <https://dx.doi.org/10.1088/2058-9565/ad5eb6>
- [61] M.-H. Hsieh and F. Le Gall, "NP-hardness of decoding quantum error-correction codes," *Phys. Rev. A*, vol. 83, p. 052331, 2011.
- [62] K.-Y. Kuo and C.-C. Lu, "On the hardnesses of several quantum decoding problems," *Quant. Inf. Process.*, vol. 19, no. 4, pp. 1–17, 2020.
- [63] P. Iyer and D. Poulin, "Hardness of decoding quantum stabilizer codes," *IEEE Trans. Inf. Theory*, vol. 61, no. 9, pp. 5209–5223, 2015.
- [64] K.-Y. Kuo and C.-Y. Lai, "Comparison of 2D topological codes and their decoding performances," in *Proc. IEEE Int. Symp. Inf. Theory (ISIT)*, 2022, pp. 186–191.
- [65] J. Chen, Z. Yi, Z. Liang, and X. Wang, "Improved belief propagation decoding algorithms for surface codes," *arXiv preprint arXiv:2407.11523*, 2024.
- [66] J. Du Crest, F. Garcia-Herrero, M. Mhalla, V. Savin, and J. Valls, "Layered decoding of quantum ldpc codes," in *2023 12th International Symposium on Topics in Coding (ISTC)*, 2023, pp. 1–5.
- [67] C. Wang, J. Harrington, and J. Preskill, "Confinement-Higgs transition in a disordered gauge theory and the accuracy threshold for quantum memory," *Annals of Physics*, vol. 303, no. 1, pp. 31–58, 2003.
- [68] C. T. Chubb, "General tensor network decoding of 2d pauli codes," 2021. [Online]. Available: <https://arxiv.org/abs/2101.04125>
- [69] J. Edmonds, "Paths, trees, and flowers," *Canadian Journal of Mathematics*, vol. 17, pp. 449–467, 1965.
- [70] D. S. Wang, A. G. Fowler, A. M. Stephens, and L. C. L. Hollenberg, "Threshold error rates for the toric and planar codes," *Quant. Inf. Comput.*, vol. 10, no. 5, pp. 456–469, 2010.
- [71] A. deMartí iOlus, P. Fuentes, R. Orús, P. M. Crespo, and J. E. Martínez, "Decoding algorithms for surface codes," *Quantum*, vol. 8, p. 1498, 2024.
- [72] S. Gounai and T. Ohtsuki, "Decoding algorithms based on oscillation for low-density parity check codes," *IEICE Trans. Fundam. Electron. Commun. Comput. Sci.*, vol. 88, no. 8, pp. 2216–2226, 2005.
- [73] S. Gounai, T. Ohtsuki, and T. Kaneko, "Modified belief propagation decoding algorithm for low-density parity check code based on oscillation," in *IEEE Veh. Technol. Conf. (VTC)*, vol. 3, 2006, pp. 1467–1471.
- [74] M. Jiang, C. Zhao, E. Xu, and L. Zhang, "Reliability-based iterative decoding of ldpc codes using likelihood accumulation," *IEEE Commun. Lett.*, vol. 11, no. 8, pp. 677–679, 2007.

- [75] J. Rosseel, V. Mannoni, V. Savin, and I. Fijalkow, "Sets of complementary LLRs to improve OSD post-processing of BP decoding," in *2023 12th International Symposium on Topics in Coding (ISTC)*. IEEE, 2023, pp. 1–5.
- [76] L. P. Pryadko, "On maximum-likelihood decoding with circuit-level errors," *Quantum*, vol. 4, p. 304, 2020.
- [77] J. Du Crest, M. Mhalla, and V. Savin, "Stabilizer inactivation for message-passing decoding of quantum LDPC codes," in *2022 IEEE Information Theory Workshop (ITW)*. IEEE, 2022, pp. 488–493.
- [78] J. du Crest, F. Garcia-Herrero, M. Mhalla, V. Savin, and J. Valls, "Check-agnosia based post-processor for message-passing decoding of quantum LDPC codes," *Quantum*, vol. 8, p. 1334, 2024.
- [79] T. R. Scruby, T. Hillmann, and J. Roffe, "High-threshold, low-overhead and single-shot decodable fault-tolerant quantum memory," *arXiv preprint arXiv:2406.14445*, 2024.
- [80] A. d. iOlius, I. E. Martinez, J. Roffe, and J. E. Martinez, "An almost-linear time decoding algorithm for quantum LDPC codes under circuit-level noise," *arXiv preprint arXiv:2409.01440*, 2024.
- [81] A. O. Quintavalle, M. Vasmer, J. Roffe, and E. T. Campbell, "Single-shot error correction of three-dimensional homological product codes," *PRX Quantum*, vol. 2, p. 020340, 2021.
- [82] O. Higgott and N. P. Breuckmann, "Improved single-shot decoding of higher dimensional hypergraph product codes," 2022. [Online]. Available: <https://arxiv.org/abs/2206.03122>
- [83] A. Ashikhmin, C.-Y. Lai, and T. A. Brun, "Quantum data-syndrome codes," *IEEE J. Sel. Area. Comm.*, vol. 38, no. 3, pp. 449 – 462, 2020.
- [84] K.-Y. Kuo, I.-C. Chern, and C.-Y. Lai, "Decoding of quantum data-syndrome codes via belief propagation," in *Proc. IEEE Int. Symp. Inf. Theory (ISIT)*, 2021, pp. 1552–1557.
- [85] K.-Y. Kuo and C.-Y. Lai, "Generalized quantum data-syndrome codes and belief propagation decoding for phenomenological noise," *IEEE Transactions on Information Theory*, pp. 1–1, 2025.
- [86] ———, "Fault-tolerant belief propagation for practical quantum memory," *arXiv preprint arXiv:2409.18689*, 2024.